THE *bps* SIGNAL: GENETIC AND BIOCHEMICAL APPROACHES FOR IDENTIFICATION

by

Emma Adhikari

A thesis submitted to the faculty of
The University of Utah
in partial fulfillment of the requirements for the degree of

Master of Science

Department of Biology

The University of Utah

May 2015

The University of Utah Graduate School

STATEMENT OF THESIS APPROVAL

The thesis of **Emma Adhikari**

has been approved by the following supervisory committee members:

Leslie E. Sieburth	, Chair	**7/21/2014** Date Approved
Gary N. Drews	, Member	**7/21/2014** Date Approved
Thomas A. Kursar	, Member	**7/21/2014** Date Approved

and by **M. Denise Dearing** , Chair/Dean of the

Department/College/School of **Biology**

and by David B. Kieda, Dean of The Graduate School.

ABSTRACT

Plants use root-to-shoot signaling to coordinate shoot development with the conditions experienced by the roots. A root-to-shoot signaling molecule had been implicated in the Arabidopsis *bypass 1* (*bps1*) mutant. The *bps1* mutant exhibits defective shoot and root growth that is associated with over-production of a root-derived signal, the *bps* signal. Our main goal is to characterize the *bps* signal chemically and work on purification steps for the identification of the *bps* signal. Our strategy was to create several mutants with altered levels of *bps* signal, fractionate extracts, test fractions for activity using a bioassay, and analyze the active the fraction using mass spectrometer.

I developed a bioassay to follow the *bps* signal, which is based on the growth-reducing activity using the *pCYCB1;1::GUS* cell cycle marker. Using the bioassay, we revealed that the *bps* signal is neither a protein nor RNA but it is a small metabolite. Using the bioassay and several SPE fractionation procedures, including C-18, HILIC, and MCX we showed that the *bps* signal is a polar, positively charged metabolite.

We used genetic and chemical inhibitor approaches to characterize the biosynthetic pathway of the *bps* signal. We showed that *bps1* mutants were resistant to 5-MT, an analog of Tryptophan (Trp). When Trp biosynthesis was limited in *bps1* mutants, by creating double mutants with *trp2* and *trp3* mutants,

leaf development was partially rescued. The rescued phenotype was restored when *trp2 bps1* double mutants were grown on media containing Trp. Using the bioassay, we further showed that *trp2 bps1* double mutants have a reduced level of the *bps* signal.

To characterize the *bps* signal chemically, we analyzed the numbers and level of compounds in *bps1*, *trp2 bps1*, and *cyp79B2 cyp79B3 bps1* mutants by HPLC using pHILIC analytical column. Analysis using negative and positive mode MS revealed that there were one and two potential *bps* signal candidates. Further fractionation of the extracts using a pHILIC semipreparative column and testing the fractions for activity revealed that a single 30-second fraction showed the *bps* signal activity. However, the compounds in the active 30-second fraction were different than the putative *bps* signal candidates obtained from pHILIC analytical column. Further fractionating the active 30-second fraction using cHILIC (pH 3.2) chromatography revealed that there were many more compounds in that fraction. Much additional work is required before we can clearly identify the *bps* signal.

TABLE OF CONTENTS

LIST OF FIGURES

LIST OF TABLES

ACKNOWLEDGEMENTS

I am especially grateful to my mentor Leslie E. Sieburth for all the support, advice, and encouragement throughout this work. I would also like to thank the members of my supervisory committee for valuable discussions of my work. I am extremely thankful to James Cox for teaching me HPLC-MS techniques and helping me to analyze the data. I am thankful to all my lab members, including D.K. Lee and Malia Deshotel, for critical discussions. I am extremely grateful to my husband Bill Pandit for his support, tolerance, and encouragement throughout my work. Chapter 2 is reprinted from Molecular Plant, Volume 6 number 1, Emma Adhikari, Dong-keun Lee, Patrick Giavalisco, and Leslie E. Sieburth, Long-Distance Signaling in *bypass1* Mutants: Bioassay Development Reveals the *bps* Signal to Be a Metabolite, Page No. 164-173. This work was supported by a grant from USDA.

CHAPTER 1

INTRODUCTION

1.1 Cell signaling

Cell signaling is a mode of communication that governs basic cellular activities and coordinates cell actions. In multicellular organisms, cells need to perceive, communicate, and correctly respond to the environment to coordinate the actions of cells, organs, and tissues. Classical signaling is triggered when a signaling molecule activates a specific receptor located on the cell surface or inside the cell. In turn, the receptor triggers a biochemical chain of events inside the cell, creating a response. Correct signaling is the basis of proper development, tissue repair, and immunity as well as normal tissue homeostasis. Signaling can occur within and between cells and different types of molecules can function as signals.

Plants are subjected to changes in their environment, e.g., light, dark, and temperature, which cause them to alter their metabolism, physiology, and development. In order to coordinate the changing environment and their development, signaling networks are required. Some plant organs perceive environmental information such as the presence of pathogens, and transmit this information so defense responses can be elevated. Several types of molecules are involved in the cellular communication in plants. Groups of signaling molecules include plant hormones, mRNAs, peptides, small metabolites, and miRNAs[1].

1.2 Signaling molecules in plants

One of the major groups of plant signaling compounds are the plant hormones (phytohormones), which include auxin, abscisic acid (ABA), cytokinin, strigolactone, gibberellins, Brassinosteroids, ethylene, salicylic acid (SA), and jasmonic acid (JA)[2]. Auxin was the first plant hormone discovered. Indole-3 acetic acid (IAA), which is chemically similar to the amino acid tryptophan, is the major naturally produced auxin. Auxin is mainly produced in the young, expanding leaves of the shoot apex and transported down the stem by a polar transport system. Auxin induces many responses, depending on the tissue, plant species, and age, including stimulating cell elongation, division, and differentiation, delaying leaf senescence, suppressing growth of lateral buds, inducing vascular tissue differentiation, promoting leaf and fruit abscission, and inducing fruit set and growth[3,4]. ABA is another plant hormone, and it functions in seed maturation processes, acquisition of drought tolerance, and dormancy. During vegetative growth, ABA is thought to be the key hormone that confers tolerance to environmental stresses, most notably drought and high salinity[5]. Cytokinin is another plant hormone that is synthesized by the biochemical modification of adenine[6]. It is generally synthesized in the roots and is translocated to the shoots via xylem. It stimulates cell division, morphogenesis of plant cells, growth of lateral buds, including release of apical dominance, and leaf expansion, and delay senescence of tissues[7,8]. Gibberellins are another plant hormone, and they are synthesized from acetyl CoA in young tissues of the shoot and the germinating seeds[9]. Gibberellins stimulate stem elongation by

stimulating cell division and elongation, stimulate bolting/flowering in response to long days, break seed dormancy, and induce germination[10] . Another plant hormone is carotenoid-derived strigolactone that is synthesized in the roots and inhibit shoot branching. It also functions environmentally to communicate with mycorrhizal fungi[11–13]. SA and JA are the major hormones in triggering pathogen resistance responses[14].

Peptides are another major group of signaling molecules that largely relay information that coordinates cell proliferation and differentiation. Two major groups of peptide signaling molecules in *Arabidopsis* are the CLAVATA3/ENDOSPERM SURROUNDING REGION (CLE) peptide family, and the EPIDERMAL PATTERNING FACTOR (EPF) family. The CLE peptide families are synthesized as precursors, and have a conserved 12-14 amino acid CLE motif at or near the C-terminus. A group of CLE peptides that are known to play an important role in stem cell maintenance include CLV3 (which functions in the shoot), CLE40 (which functions in roots), and CLE 41 (which functions in vascular meristem). The EPF family of peptides plays a predominant role in patterning the leaf epidermis. Four EPF family members have been characterized with respect to stomata development: EPF1, EPF2, STOMAGEN, and CHALLAH (CHAL). Collectively, these peptides influence both the frequency and orientation of asymmetric cell division that create guard cells and also enforce patterning rules that ensure that two stomata are not in direct physical contact[15].

Reactive oxygen species (ROS), which include hydrogen peroxide (H_2O_2), superoxide radical (O_2^-), hydroxyl radical (OH^-), and singlet oxygen ($^1O_2$), act as signaling molecules. Chemically, ROS can be highly detrimental to cellular function, but genetic evidence suggests that ROS can also act as a plant-signaling molecule. For example, H_2O_2 production is triggered during abiotic stress. When ROS concentration is increased, it acts as a signal by modifying the expression of defense genes. The change in the gene expression occurs due to the oxidation of components of the signaling pathway that result in the activation of the transcription factors[16]. Additional roles for ROS include cell-cell and long-distance communication in response to pests, mechanical wounding, heat, cold, high-intensity light, and salinity stress[17]. ROS accumulation is required to propagate information long distances under these diverse environmental stimuli. ROS-based communication is mediated by superoxide generated by RESPIRATORY BURST OXIDASE HOMOLOG D (RBOHD) enzyme and its reactive derivatives or both. ROS produced by RBHOD travels along the plant's stem and mediates several responses, including transcriptional regulation of target genes[17].

1.3 Intra-organ signaling

Signaling within organs is integral for the coordinated behavior of cells in the community that makes up an organ. Signaling molecules like peptides, small RNAs, and phytohormones serve an important function in intra-organ communication. Transport of this group of signaling molecules occurs through symplastic and apoplastic pathways. The symplast is the area inside cells and

symplastic movement includes transport through plasmodesmata, which are plasma membrane-lined pores that cross cell walls of adjacent cells and thus connect their cytoplasms, allowing cell-cell communication. Signaling molecules like mobile protein, small interfering RNAs, mRNAs move via plasmodesmata. Apoplast is the area outside the cell and apoplastic movement is transport through the cell wall. Intra-organ cellular communication occurs through apoplast and the movement of phytohormone auxin is a classical example[18].

Examples of peptides that play an important role in intra-organ signaling include, CLV3, CLE40, and CLE41. These peptides play an important role in a similar manner in the maintenance of shoot, root, and vascular stem cell population. The niches of the shoot and root meristems coordinate the fine balance of stem cell maintenance. The shoot meristem consists of the organizing center (OC) and its adjacent cells and the root meristem consists of the quiescent center (QC) and its adjacent cells. The OC and QC express functionally equivalent homeobox transcription factors WUSCHEL (WUS) and WOX5, respectively, and these confer stem cell identity to the adjacent cells. In the shoot meristem, cells adjacent to the OC signal back to the OC by secreting CLAVATA 3 (CLV3) peptide. CLV3 is expressed in a small cell group of the apical layers of the shoot meristem and limits WUS activity by restricting its expression to the OC[19,20]. In the root meristem, CLE 40, a peptide closely related to CLV3, has been implicated in promoting differentiation of the distal root meristem. CLE40 from the differentiated root cells provides a negative feedback signal that balances stem cell proliferation to regulate WOX5 expression in the

QC[21]. In the vascular meristem, stem cells named procambial cells proliferate and their progeny differentiate into xylem and phloem cells. CLE 41 is secreted from the phloem and both promotes proliferation of procambial cells while at the same time suppressing differentiation of xylem cells, hence maintaining the stem cell population. CLE 41 positively controls the expression of WUSCHEL-related HOMEOBOX4 (WOX4). WOX4 is expressed in the procambium and cambium cells and controls maintenance of the vascular cambium but not the differentiation into Xylem[22].

Another group of molecules that signal between cells are the small RNAs. Examples of signaling small RNAs include MIR165, MIR 166, and tasi-ARFs. In the root meristem, *MIR165A* and *MIR166B* are transcribed in the endodermis. These miRNA move radially, through plasmodesmata, to the stele periphery. In the stele periphery, they cleave mRNAs that encode PHABULOSA (PHB), a class III homeodomain leucine zipper (HD-ZIP III) transcription factor. *PHB* is therefore restricted within the stele center and it promotes protoxylem differentiation resulting in proper xylem patterning[23]. In the shoot meristem, conserved tasi-RNAs, termed tasi-ARFs, are produced in the upper adaxial side of the leaves. These RNAs are transported to the lower abaxial side of the leaf. This results in a gradient of small RNAs that pattern the abaxial determinant AUXIN RESPONSE FACTOR 3[24].

1.4 Inter-organ signaling

During plant development, distantly located organs such as root and shoot must communicate with each other so that the organism can develop as a

coordinated whole and adapt to the changing environment. For example, plants use their roots to acquire essential mineral nutrients from the rhizosphere; these nutrients are then translocated to shoots for growth and reproduction. Shoots produce sugars, which are then transported to the roots[25]. Plants need to respond to external stimuli as a whole organism, particularly during stress. Long-distance communication between roots and shoots is essential to coordinate the adaptive response in the whole body of the plant. The vascular system, which consists of two conducting tissues, phloem and xylem, provides routes for long-distance movement. Water, together with sugars, amino acids, and inorganic nutrients are distributed throughout the plant, via the xylem. Signaling molecules like mobile peptides and phytohormone auxin move through the xylem. Phloem is the living tissue of the vascular system and signaling molecules like mobile proteins, peptides, mRNAs, and small RNAs transport through the phloem[26].

1.4.1 Root-to-shoot signals

Roots are positioned where they learn information about soil conditions that have important implications for shoot physiology. This information is conveyed to the shoot through signaling molecules that are transported long distance. A classical example comes from chemical signaling when roots are exposed to drought conditions. As the soil becomes dry, root-sourced signals are transported via the xylem to the leaves and result in reduced water loss and decreased leaf growth[27]. However, the identity of the compound is not known. Although not necessarily related to the drought response, examples of signaling molecules that move from the root to the shoot are the phytohormones

strigolactone, cytokinin, and ABA. Strigolactone, which is synthesized in roots, controls shoot branching[12]. Cytokinin has been implicated in communicating the nitrogen status from the root to the shoot and regulating senescence[8]. Another plant hormone, abscisic acid (ABA), is thought to communicate drought conditions from the root to the shoot[5].

Another example of root-to-shoot signaling is phosphorous (P) signaling. P is an essential macronutrient, as it is present in a majority of a cell's molecular constituents, including DNA, RNA, proteins, lipids, sugars, ATP, ADP, and NADPH. For proper growth and development, adequate P must be supplied from the soil in the form of inorganic phosphorous (Pi), which is done by the plant's root system. When Pi availability is limited, root-derived Pi deficiency signals are generated and transported, via the xylem, to the shoot[28]. The signals are then perceived by shoot-specific sensors, which trigger adaptive responses within shoots. Currently, the root-derived signal is not known, but candidates include Pi itself, phytohormone auxin, ethylene, cytokinin, abscisic acid, gibberellins, and strigolactone; along with sugars, miRNA and Ca^{+}[29]. The responses in the shoot include reduced photosynthetic activity, increased accumulation of sugars, and retardation of shoot development[28].

1.4.2 Shoot-to-root signals

Just as root-to-shoot signaling provides the shoot with vital information about the rhizosphere, there are also signaling molecules that move from the shoot to the root, again to coordinate the activities of these two organ systems. As with root-to-shoot signaling, the chemical nature of these signaling molecules

is diverse, and includes mRNA, miRNA, and small metabolites.

An example of shoot-to-root signaling comes from the potato plant, *Solanum tuberosum*, where the timing of tuber formation on the stolen tip is coordinated with leaf growth. The signaling molecule that activates tuber formation is the mRNA for a transcription factor, *StBEL5*. Tuber forms from the sub-apical region of the stolen tip; stolen is a specialized stem that grows horizontally and under favorable conditions. The signaling molecule that activates tuber formation is the mRNA for a transcription factor, *StBEL5*. *StBEL5* mRNA originates in the leaf and its mRNA accumulates in response to short-day photoperiods. The mRNA moves to the stolen through the phloem. Translation of *StBEL5* mRNA occurs on site and together with its protein partner, POTH1, it auto-regulates its own transcription. *StBEL5* mRNA mediates tuber development in the stolen tip via modulating auxin levels. *StBEL5* mRNA functions in targeting auxin synthesis genes and auxin signaling processes[30,31].

MicroRNAs also play an important role in communicating shoot nutrient conditions to the root. As discussed in the previous section, low Pi availability in the soil induces expression of genes in the shoot; one of these is MiR399. When plants experience phosphate (Pi) deficiency, miR399 is expressed in the shoot and is transmitted through the phloem to the root. In the root, miR399 regulates expression of *PHOSPHATE 2* (*PHO2)* and its transcripts drop by 8-fold. Due to the drop of *PHO2* transcripts, Pi starvation-induced genes *ATIPS1*, *AT4*, and Pi transporters *Pht1;8* and *Pht1;9* cannot be repressed, hence allowing Pi-uptake[32,33].

A final example of shoot-to-root signaling, this time using a metabolite as a signal, is 'shoot derived inhibitor' (SDI) in soybean. The number of root nodules formed by legumes is tightly controlled via a complex root-to-shoot-to-root signaling loop termed autoregulation of nodulation. This regulatory loop involves peptide hormones, receptor kinases, and small metabolites. A CLE peptide hormone that is highly similar to CLV3 is produced in the root with the development of nodule primordia and nitrogen fixation. This signal is transported long-distance to the leaf, via the xylem, triggering the production of a shoot-derived inhibitor, named 'SDI'. SDI moves down into roots via the phloem where it suppresses further nodulation. Although SDI has not been identified chemically, recent work in soybean has shown that it is likely to be a metabolite. SDI is small (<1 kDa), heat stable, and unlikely to be an RNA or protein[34,35].

1.5 Implication of unknown signaling pathways

Physiological and genomic experiments suggest that there are signaling molecules that are yet to be identified. One of the examples comes from phosphorous (Pi) signaling. Pi is one of the essential macromolecules that is normally taken from the soil and, under certain environmental conditions, Pi may be limited in the soil. To manage the low Pi availability, roots and shoots react cooperatively to enhance the acquisition of external Pi. Signal from the roots travels to the shoot and induces shoot-specific Pi deficiency responses, such as reduced photosynthetic activity, increased accumulation of sugars, and retardation of shoot development. Currently, the nature of the signaling molecule remains largely unknown[29,36].

The best physiological example of an unknown signaling molecule comes from the studies using split root experimental design, where root system of an individual plant was split between two containers. The experiment indicated that there is an unknown root-to-shoot signal controlling leaf development that is evoked by drought. In experiments using maize (*Zea Mays* L.), the root system was divided between two containers and the soil in one container was allowed to dry while the other container was kept well watered. Soil drying resulted in 35% and 15 % inhibition of leaf elongation and expansion rates, respectively. Nevertheless, leaf water potential did not decline, suggesting that leaf growth inhibition was not a direct result of water scarcity. Instead, the data suggested that inhibition arose from a root-derived signal. The drought-exposed portion of the root was thought to be the source of the inhibitor of shoot growth, because when the dried root was excised, the shoot rapidly resumed normal growth rates[37]. This provides strong evidence for the existence of root-derived signal and the identity of this signal is currently unknown.

All living systems perceive and process information from chemical signals via cell surface receptors. In animals, the family of receptor tyrosine kinases (RTKs) mediates many signaling events at the cell surface. Similar in structure to the animal RTKs, plant receptor-like kinases (RLKs) can act as signaling molecules. Plant RLKs are a class of transmembrane kinases with a predicted signal sequence, single transmembrane region, and cytoplasmic kinase domain. The *Arabidopsis* genome encodes more than 600 RLKs, but ligands for only a few RLKs have been identified. Some of the characterized RLKs functions

include brassinosteroid signaling (BRI1), meristem development (CLV1), pathogen detection (FLS2), and control of leaf development (Crinkly4)[38,39]. However, most RLKS have to be yet characterized functionally, which suggests that many more novel ligands await discovery.

1.6 *bypass* signaling pathway

The *Arabidopsis bypass1* (*bps1)* mutant was discovered in a screen as a recessive mutant with leaf vein-patterning defects. The *bps1* mutant is smaller than the wild type, and shows leaf development arrest and abnormal root development. The *bps1* rosettee leaves undergo developmental arrest soon after initiation and under most growth conditions, they remain small and radialized. The *bps1* primary root ceases elongation and differentiation extends to the root apex. Lateral roots, which appear to initiate normally, also arrest in a manner similar to the primary root[40] (Fig. 1.1A). The affected gene, *BYPASS1*, encodes a plant-specific protein with a single domain that is functionally uncharacterized. A root-derived signal that is necessary and sufficient to arrest shoot growth was implicated in *bps1* mutants[40]. When *bps1* mutant roots are intact, shoot arrest occurs shortly after germination. However, in experiments where the root is removed, *bps1* leaf development is restored. This suggested that the *bps1* roots might produce a mobile compound that moved up to the shoot and was causing shoot arrest. Grafting studies tested this idea. When *bps1* roots were grafted to wild type shoots, wild type shoot growth arrested. Taken together, the root excision and grafting experiment indicated that *bps1* roots were both necessary and sufficient to arrest leaf development. These

experiments led us to postulate a model that describes the *bps1* mutant (Fig. 1.1B). We propose that the *bps1* root produces a mobile substance, which we call the *bps* signal, and that this substance moves up to the shoot and arrests leaf development, and the same molecule also affects root development. Because *bps1* mutants are recessive, the normal BPS1 activity appears to prevent excess production of the *bps* signal. We tested the root as the source of the *bps* signal production by preventing root growth in *bps1* mutants. Postembryonic root growth and development requires glutathione (GSH), and γ-glutamylcysteine synthetase is the first enzyme that is required for the GSH biosynthesis[41]. We blocked root growth in *bps1* mutants by growing them on media containing L-buthionine sulfoximine (BSO), an inhibitor of γ-glutamylcysteine synthetase. We blocked root growth genetically by generating double mutants between *bps1* and *root meristemless1-1* (*rml1-1*), which has a defect in the gene encoding γ-glutamylcysteine synthetase and lacks postembryonic root development[42,43]. *rml1-1 bps1-2* double mutants and the *bps1* mutants grown on BSO-supplemented medium showed partial rescue of the leaf development[43]. Together with the grafting data, these results provide strong support for postgermination growth arrest arising because of a non-cell-autonomous compound produced by the *bps1* root. We have called this compound the *bps* signal.

1.7 Hypothesis and goals

We postulate that the *bps* signal is a plant hormone that is produced in wild type plants and that this putative hormone is over-produced in the *bps1*

mutants. Further, the similarity between responses of a wild type shoot to partial root drying and the responses of shoots to the *bps* signal suggests that its normal function might be related to drought and osmotic stress. If the *bps* signal is a novel hormone, its chemical identification would be a significant contribution to plant biology. My goal is to characterize the *bps* signal chemically. Once it is identified, we can work to understand how the signal affects plant growth and how normal plants use this signal to coordinate development. Extracts from wild type plants subjected to abiotic stress conditions can be analyzed to determine whether its synthesis is evoked in normal plants under conditions known to provoke root-to-shoot signaling (e.g., drought or osmotic stress).

In my project, I have used genetic and biochemical approaches to narrow down the number of candidates for the *bps* signal. I developed a bioassay to test extracts for the presence of the *bps* signal, which is described in Chapter 2. Chapter 3 describes the production of genetic resources to aid in *bps* signal identification. These are various double mutants or chemical treatments that appear to either decrease the *bps* signal in *bps1* mutants, or reduce the production of secondary metabolites that could interfere with *bps* signal identification. Chapter 4 describes my biochemical analysis of extracts from these various genetic resources, and progress toward HPLC-MS identification of the *bps* signal.

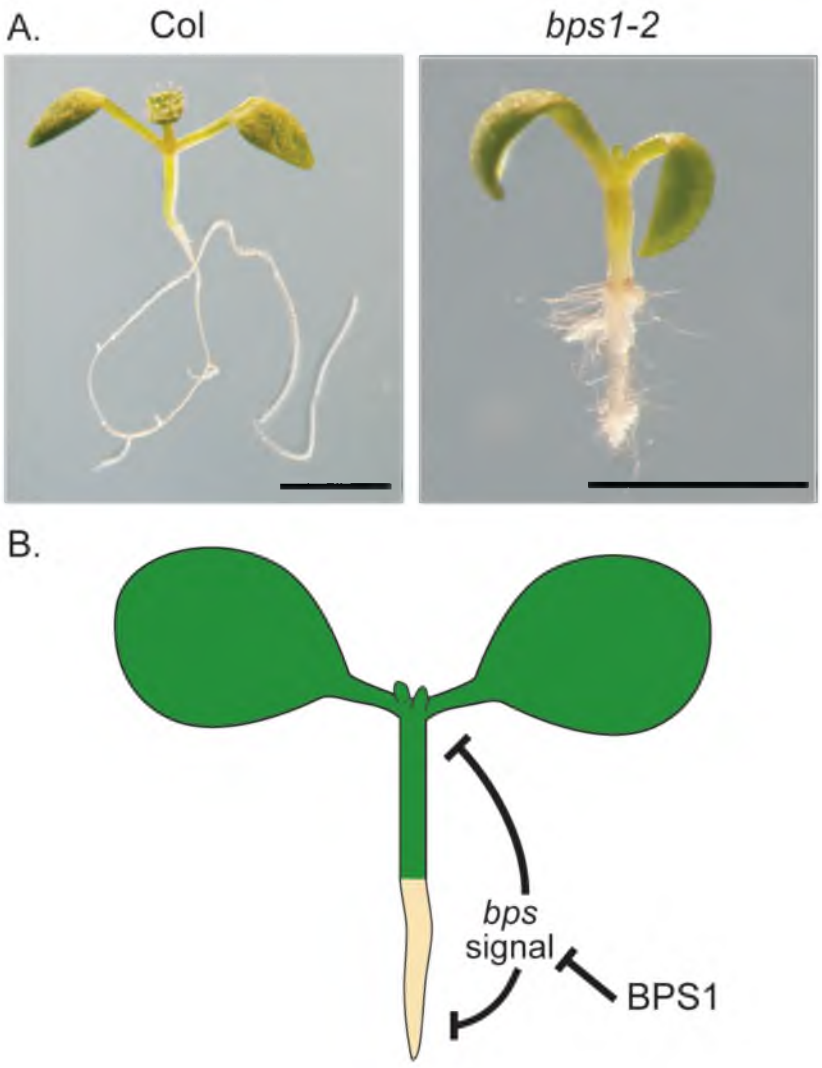

Figure 1.1: *bps1* mutants have arrested leaf growth and altered root development. (A) Phenotype of 7-day wild type and *bps1* mutant. Wild type has an elongated root and two expanding leaves with trichome. In contrast, *bps1* homozygous mutant is small, the cotyledons fail to fully expand, the leaves arrest as radialized primordia, and the roots are short, with differentiation extending to the root apex. (B) Model for BPS1 action as a negative regulator of a mobile root-derived signaling molecule, *bps* signal. Size bars = 2mm.

CHAPTER 2

LONG-DISTANCE SIGNALING IN *bypass1* MUTANTS: BIOASSAY DEVELOPMENT REVEALS THE *bps* SIGNAL TO BE A METABOLITE

Reprint with permission from Molecular Plant

Adhikari et al.,(2013), Vol 6(1), 164–73.

Molecular Plant • Volume 6 • Number 1 • Pages 164–173 • January 2013 RESEARCH ARTICLE

Long-Distance Signaling in *bypass1* Mutants: Bioassay Development Reveals the *bps* Signal to Be a Metabolite

Emma Adhikari[a], Dong-Keun Lee[a], Patrick Giavalisco[b] and Leslie E. Sieburth[a,1]

a Department of Biology, University of Utah, Salt Lake City, UT 84112, USA
b Max Planck Institute of Molecular Plant Physiology, 14476 Potsdam-Golm, Germany

ABSTRACT **Root-to-shoot signaling is used by plants to coordinate shoot development with the conditions experienced by the roots. A mobile and biologically active compound, the *bps* signal, is over-produced in roots of an *Arabidopsis thaliana* mutant called *bypass1* (*bps1*), and might also be a normally produced signaling molecule in wild-type plants. Our goal is to identify the *bps* signal chemically, which will then allow us to assess its production in normal plants. To identify any signaling molecule, a bioassay is required, and here we describe the development of a robust, simple, and quantitative bioassay for the *bps* signal. The developed bioassay follows the growth-reducing activity of the *bps* signal using the *pCYCB1;1::GUS* cell cycle marker. Wild-type plants carrying this marker, and provided the *bps* signal through either grafts or metabolite extracts, showed reduced cell division. By contrast, control grafts and treatment with control extracts showed no change in *pCYCB1;1::GUS* expression. To determine the chemical nature of the *bps* signal, extracts were treated with RNase A, Proteinase K, or heat. None of these treatments diminished the activity of *bps1* extracts, suggesting that the active molecule might be a metabolite. This bioassay will be useful for future biochemical fractionation and analysis directed toward *bps* signal identification.**

Key words: hormone biology; metabolic regulation; physiology of plant growth; secondary metabolism/natural products; signaling, organismal level; development.

INTRODUCTION

Mobile signaling molecules play critical roles in plants. During normal development, mobile signals coordinate processes both within organs and between organs, and, following exposure to stresses, mobile signaling molecules coordinate responses throughout the plant. These are vital functions, and understanding plants requires a full understanding of both the signaling molecules and their biological functions.

Many plant signaling molecules are understood in detail. For example, the population of stem cells within the shoot apical meristem (SAM) is regulated by two mobile signals: the CLV3 peptide and the WUS transcription factor (Schoof et al., 2000; Rojo et al., 2002; Müller et al., 2006; Yadav et al., 2011). Insight into how the shoot's stem cells are maintained required identification of these mobile signals. As another example, the mobile hormone, auxin, coordinates cell identity specification within the developing root meristem (Furutani et al., 2004; Blilou et al., 2005; Galinha et al., 2007; Dubrovsky et al., 2008). Strigolactone is also a mobile signaling molecule that coordinates developmental events in the root and shoot. Strigolactone is largely synthesized in roots, and its transport to shoots regulates branching by arrest of axillary meristems (Sorefan et al., 2003; Booker et al., 2005; Bennett et al., 2006; Gomez-Roldan et al., 2008; Umehara et al., 2008).

These known signaling pathways reveal an already complex network of signals and responses (Liu et al., 2010; Vercruyssen et al., 2011; Naseem et al., 2012). However, both genetic and physiological studies indicate the existence of additional and as-yet-unidentified signaling molecules (Delves et al., 1986; Gowing et al., 1990; Davies and Zhang, 1991; Van Norman et al., 2004; Anastasiou et al., 2007; Eriksson et al., 2010). To truly understand how plants function, new signaling molecules must be identified and their interactions with established pathways clarified.

[1] To whom correspondence should be addressed. E-mail Sieburth@biology.utah.edu.

doi:10.1093/mp/sss129

Received 21 September 2012; accepted 27 October 2012

An unknown mobile signaling molecule was implicated by characterization of the *bypass1* (*bps1*) mutant of *Arabidopsis* (Van Norman et al., 2004). This mutant shows severe root and shoot growth defects (Figure 1A), both of which arise due to a non-cell-autonomous signal generated within the roots, which we refer to as the *bps* signal. Grafting and root cut experiments revealed that the shoot is capable of normal development when separated from the root (Van Norman et al., 2004, 2011), which indicated that the *bps1* root was necessary for shoot developmental arrest. Grafting revealed that the *bps1*-generated signal was also sufficient for shoot arrest, as graft chimeras that combined a wild-type scion with a *bps1* rootstock showed arrested leaf development. Together, these analyses led us to formulate a model proposing that BPS1 functions to modulate synthesis of a mobile compound that mediates coordinated development between the shoot and root.

The *BYPASS1* gene was identified through positional cloning (Van Norman et al., 2004). It encodes a protein of unknown function, and has no sequence motifs suggestive of its intracellular localization. However, *BPS*-like genes are highly conserved in plant genomes, and are typically present as a multi-gene family. In *Arabidopsis*, the three *BPS* genes all contribute to negative regulation of the *bps* signal (Lee et al., 2012), and earlier production of the *bps* signal in the *bps* triple mutant leads to arrest during early embryogenesis. The broad expression patterns of *BPS* genes suggest that the *bps* signal has the potential to be used in signaling scenarios beyond root-to-shoot communication.

Our long-term goal is to elucidate the entire *bps* signaling pathway, and chemical and structural identification of the *bps* signal is a critical next step. In previous studies, we determined that the synthesis of the *bps* signal required an intact carotenoid biosynthetic pathway (Van Norman and Sieburth, 2007). The simplest interpretation of this observation is that a carotenoid serves as the biosynthetic precursor of the *bps* signal. Two carotenoid-derived signaling molecules are already known: abscisic acid and strigolactone. Genetic analysis has allowed us to rule out both of these as candidates for the *bps* signal. Because blocking carotenoid biosynthesis leads to plastid photo-oxidation, and any plastid-localized reaction is likely to be disrupted, the carotenoid requirement for *bps* signal synthesis might be either direct or indirect. Identification of the *bps* signal will be necessary for understanding the root-to-shoot signaling shown in this mutant, and it will allow us to analyze wild-type plants to determine the conditions under which they normally produce this compound.

In this study, we describe the development of a robust bioassay for detection of the *bps* signal. This assay responds to the *bps* signal whether supplied through a graft or in crude extract. Extract analysis suggests that the mobile molecule might be a small molecule, likely a common metabolite or an unusual side-product from a metabolic pathway. The bioassay reported here represents an important step towards identification of this mysterious compound.

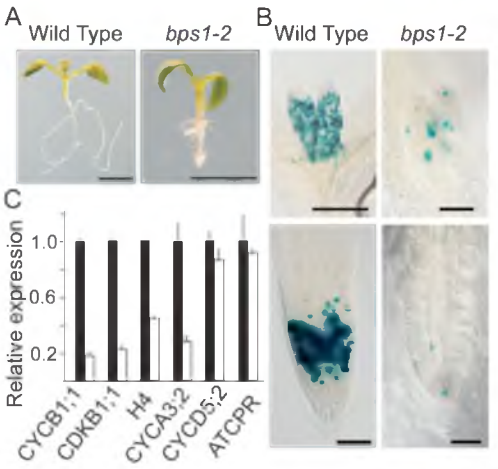

Figure 1. Growth Arrest of *bps1* Mutants Is Associated with Altered Cell Division.

(A) Seven-day-old wild-type (Col-0) and *bps1-2* seedlings.

(B) Expression pattern of *pCYCB1;1::GUS* in 4-day-old wild-type (Col) and *bps1-2* mutant leaf primordia (top) and roots (bottom).

(C) Relative expression of the cell cycle genes expressed in G2/M, S, and G1 phases of the cell cycle. Solid bars represent wild-type and open bars represent *bps1*. Error bars show SEM. Size bars: 2 mm in (A) and 50 µm in (B).

RESULTS AND DISCUSSION

Cell Division Is Altered in *bps1* Mutants

The *bps1* mutant exhibits severe shoot and root growth defects. Its small size appears to be the result of decreased cell division, as the G2/M cell cycle marker, *pCYCB1;1::GUS* (Colón-Carmona et al., 1999), is expressed in fewer cells in the *bps1* mutant (Figure 1A and B; Van Norman et al., 2011). To test whether *pCYCB1;1::GUS* faithfully represented *bps1* cell cycle status, we used real-time qRT–PCR to analyze transcript levels of six cell cycle genes: *CYCB1;1*; *CYCLIN B DEPENDENT KINASE* (*CDKB1;1*); *HISTONE H4* (*H4*); *A-TYPE CYCLIN* (*CYCA3;2*); *D-TYPE CYCLIN* (*CYCD5;2*); and *ARABIDOPSIS CELL-PROLIFERATION-RELATED GENE* (*ATCPR*) (Hemerly et al., 1992; Ferreira et al., 1994; Segers et al., 1996; Potuschak and Doerner, 2001; Boudolf et al., 2004; Menges et al., 2005; Dhondt et al., 2010; Figure 1C). Consistently with the *pCYCB1;1::GUS* reporter, endogenous *CYCB1;1* mRNA was also strongly depleted in the *bps1* mutant. Expression of *CDKB1;1*, another G2/M phase transcript, and the S-phase-specific transcripts *Histone H4* and *CYCA3;2* were also strongly reduced in *bps1* mutants. By contrast, *bps1* mutants showed normal levels of the G1-phase RNAs (*ATCPR*, *CYCD5;2*). The depletion of G2/M and S-phase transcripts links the small stature of *bps1* mutants to reduced cell division, and suggests that the *bps* signal leads to cell cycle arrest, probably at G1.

The *bps* Signal Can Pass through Agarose

Because the *pCYCB1;1::GUS* reporter provides a simple and quantitative readout of growth arrest, we explored whether it would be suitable as a bioassay for the *bps* signal. The clearest evidence that the *bps* signal was non-cell-autonomous came from grafting experiments, where a *bps1* root was found to be sufficient to induce arrest of wild-type leaf growth (Van Norman et al., 2004). We therefore extended the graft analyses to see whether wild-type leaf primordia showed reduced *pCYCB1;1::GUS* expression following grafting to *bps1* roots. Establishment of graft chimera involves generation of callus by both the scion and the rootstock, followed by differentiation of vascular tissues, and these processes proceed over many days (Moore, 1984; Wang, 1996; Flaishman et al., 2008; Yin et al., 2012). Because traditional grafting is unsuitable for measuring rapid signal transduction, we developed a transient micrografting method to analyze rapid responses. This method was based on *Arabidopsis* micrografting (Turnbull et al., 2002), but, instead of physical contact between scion and rootstock, we embedded them in a small agarose block (Figure 2A). Wild-type scion carrying the *pCYCB1;1::GUS* transgene were embedded in agarose blocks and then either left uncoupled, coupled to a wild-type (Col-0) rootstock, or coupled to the *bps1-2* root. After 24 h, the scion were GUS-stained and the number of *pCYCB1;1::GUS*-stained cells in leaf primordia were counted.

The wild-type leaf primordia showed variable numbers of *pCYCB1;1::GUS*-stained cells, whether exposed to wild-type roots, no roots, or the *bps1* root. To display the full extent of these variable numbers, we plotted the data in box plots (Figure 2). The vertical bar extends to the highest and lowest data points, the box extends between the 25th and 75th percentiles, and it is bisected at the median. Wild-type *pCYCB1;1::GUS* scion coupled to a wild-type root, or to no root, showed very similar ranges of cell counts. However, wild-type *pCYCB1;1::GUS* scion coupled to the *bps1-2* rootstock produced leaf primordia with dramatically fewer *pCYCB1;1::GUS*-stained cells (Figure 2B and 2C). These results indicate that the leaves of the wild-type scion responded to the *bps1* root. Because *bps1* roots appear to produce a mobile signal, the *bps* signal, these results suggest (1) that *pCYCB1;1::GUS* expression responds rapidly to the *bps* signal (in less than 24 h) and (2) that the *bps* signal can pass through the 0.8% agarose (in water), and so is likely to be a hydrophilic molecule.

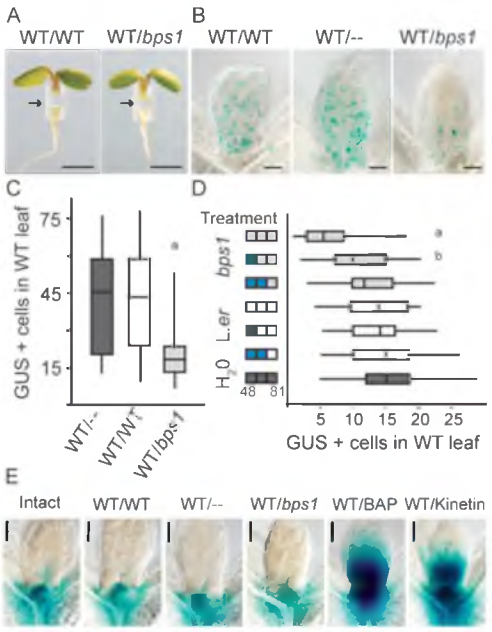

Figure 2. The *bps* Signal Causes Reduced Wild-Type Leaf Cell Division whether Transmitted through Grafts or Applied through Extracts, But It Does Not Activate the *pARR5::GUS* Cytokinin Reporter.
(A) Transient micrografts with 4-day-old wild-type (WT) *pCYCB1;1::GUS* scion coupled to WT or *bps1-1* rootstocks. Arrows point to the agarose plug.
(B) Expression of *pCYCB1;1::GUS* in WT leaf primordia 24 h after micrograft coupling.
(C) Box and whisker plots of *pCYCB1;1::GUS*-stained cells in WT leaf primordia following transient micrografts (n = 32 for each micrograft couple). Boxes delineate the data points falling between 25% and 75%, the line bisecting the box shows the median, and the whiskers indicate the highest and lowest data point.
(D) Test of crude extracts on WT leaf cell division. Strategy for extracts addition is to the left. Box plots show *pCYCB1;1::GUS*-stained cells in WT leaf primordia treated with water or extracts (n = 21 for each sample).
(E) *pARR5::GUS* expression in WT leaf primordia 24 h after micrograft coupling to WT or *bps1* rootstocks; positive controls used 1 μM cytokinin (BAP and Kinetin) supplied in the agarose plug (n = 16, each treatment). Results with significant differences are labeled with letters a and b (Mann-Whitney U-test; a = $P < 0.005$ and b = $P < 0.05$). Size bars: 1.0 mm in (A) and 50 μm in (B, E).

The *bps* Signal Is Not Cytokinin

Cytokinin is also known to influence cell division (Riou-Khamlichi et al., 1999) and to move from roots to shoots (Aloni et al., 2005), so we used a grafting approach to test whether the *bps* signal could be cytokinin. As scions, we used wild-type shoots carrying the primary cytokinin response marker, *pARR5::GUS* (D'Agostino et al., 2000). This marker has previously been shown to be activated by 2.5 μM BAP supplied through the media, and we found that shoots carrying *pARR5::GUS* responded strongly to cytokinin (1 μM BAP and Kinetin) supplied in the agarose of a micrograft tube (Figure 2E). By contrast, shoots carrying *pARR5::GUS* that were transiently grafted to either wild-type or the *bps1* roots showed no elevation of *pARR5::GUS* expression. These data indicate that the *bps1* roots do not supply excess cytokinin to the shoot, and are consistent with the *bps* signal being a novel mobile compound.

Extracts from *bps1* Mutants Diminish Cell Division in Wild-Type Leaves

Because our long-term goal is to identify the *bps* signal biochemically, it is essential that our bioassay is responsive to the *bps* signal applied as semi-purified extracts. We therefore tested whether extracts from *bps1*, but not the wild-type, could replicate the *pCYCB1;1::GUS*-staining expression responses observed in the transient micrograft assay. Because transmission of the *bps* signal across an agarose matrix suggested that it was a hydrophilic molecule, we prepared crude extracts using a water–methanol–chloroform extraction protocol to separate polar from hydrophobic molecules (Giavalisco et al., 2008). As starting material, we used both *bps1-1* seedlings and its corresponding wild-type, Landsberg *erecta* (L. *er*). The resulting crude polar extracts (methanol–water fraction) were then tested for *bps* signal activity by applying them to wild-type seedlings carrying *pCYCB1;1::GUS*.

Extract was supplied to wild-type *pCYCB1;1::GUS* seedlings grown in microtiter dishes at 48, 59, and 70 h (11-h intervals; see strategy in Figure 2D), and the effect of these treatments on *pCYCB1;1::GUS* staining in the leaf primordia was compared. Those seedlings supplied with only water or with combinations of water and wild-type extracts showed similar numbers of *pCYCB1;1::GUS*-stained cells in their leaf primordia. Wild-type seedlings supplied with only a single *bps1* extract 11 h before staining also showed numbers of *pCYCB1;1::GUS*-stained cells that were similar to the controls. However, wild-type seedlings provided with two or three aliquots of *bps1* extract showed significantly reduced numbers of *pCYCB1;1::GUS*-stained leaf cells. These responses indicated that the crude polar extract contained the *bps* signal and that the extract was able to affect *pCYCB1;1::GUS* expression.

The responses of wild-type leaf cell division to the *bps1* root (in transient micrografts) and to extracts from *bps1* mutants were similar, suggesting that *pCYCB1;1::GUS* provides a useful readout for the *bps* signal. Interestingly, supplying polar extracts required repeated treatments to achieve GUS-staining repression in the leaf; this might reflect a longer path for the extracts to travel, namely uptake through the roots prior to transport to the leaf. Alternatively, it is possible that the transient micrograft was more efficient at repressing the *pCYCB1;1::GUS* activity because the *bps1* root provides a continuous supply of the *bps* signal. Regardless of why the multiple treatments were required, the observation that *bps1* extracts, and not the extracts from the wild-type, conferred cell cycle repression indicated that the water–methanol extract contains the expected polar *bps* signal.

Root-Based Bioassay

Identification of the *bps* signal based on its activity requires a bioassay that is quick and requires small amounts of extract. However, because leaf responses to extracts were neither fast nor extract-frugal, we explored the possibility of carrying out the bioassay using *Arabidopsis* roots. Roots show strongly reduced numbers of *pCYCB1;1::GUS*-expressing cells in *bps1* mutants (Figure 1B), and the root defects arise from the same mobile compound as leaf defects (Van Norman et al., 2004), so we anticipated that they would respond to the polar methanol–water extracts. Moreover, we reasoned that the predictable root meristem size (Dolan et al., 1993) might facilitate comparisons of extract activity between different experiments.

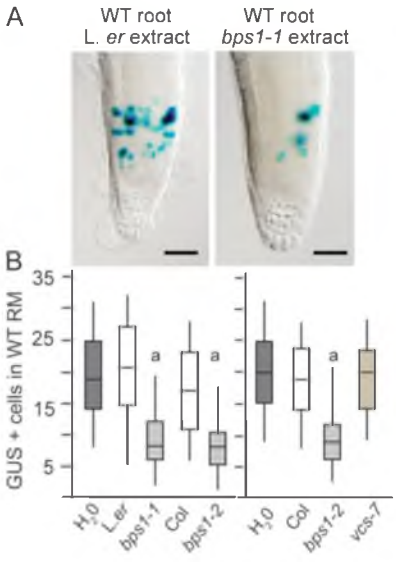

Figure 3. Wild-Type (WT) Root Meristem Cell Division Is Sensitive to the *bps* Signal.
(A) WT *pCYCB1;1::GUS*-stained roots treated with WT or *bps1* extracts.
(B) Numbers of *pCYCB1;1::GUS*-stained cells in WT roots treated with water or extracts. The letter 'a' represents a statistical significance $P < 0.005$ (Mann-Whitney U-test). Size bars: 50 μm.

To test whether wild-type roots responded to *bps1* extracts, we carried out a 17-h incubation of wild-type *pCYCB1;1::GUS* seedlings with wild-type or *bps1* extracts, and then assessed the number of GUS-positive cells in the root meristem. Wild-type roots supplied with wild-type extracts looked similar to controls (water), whereas those supplied with *bps1* extracts showed fewer GUS-stained cells (Figure 3A). We tested extracts from two *bps1* alleles, *bps1-1* and *bps1-2*, and their corresponding wild-type (L. er and Col-0, respectively); extracts from both mutants elicited a strong reduction in *pCYCB1;1::GUS* staining, while both L. *er* and Col-0 wild-type extracts had no effect (Figure 3B). This ability to reduce *pCYCB1;1::GUS* expression using *bps1* extracts was not merely a consequence of their small size, as the bioassay response to extracts from *varicose-7*, a mutant similar in size to *bps1* (Goeres et al., 2007), was similar to that for wild-type extracts

(Figure 3B). Finally, wild-type roots show a broad distribution of *pCYCB1;1::GUS*-stained cell numbers per root, regardless of whether they were provided with water or wild-type extracts (Supplemental Figure 1). The distribution, though, was significantly skewed to the low range following provision with *bps1* extracts. These data therefore support that the root *pCYCB1;1::GUS* activity is a useful readout for the activity of the *bps* signal.

As an additional test for whether the extracts conferred a *bps1*-like response, we looked for other *bps1*-like features in the wild-type roots treated with *bps1* extracts. QC46 is a quiescent center GUS marker (Sabatini et al., 1999); *bps1* mutants fail to express this marker and they also produce misshapen columella cells that lack starch granules (Figure 4A). We treated wild-type seedlings carrying QC46 with polar extracts prepared from the wild-type and *bps1* mutants. Up to three treatments were provided, and roots were analyzed for columella starch granules and QC46 expression. We found strong QC46 expression in all the wild-type seedlings, regardless of whether wild-type or *bps1* extracts were supplied. However, we observed fewer starch-containing columella cells in seedlings provided with the *bps1* extract three times (Supplemental Figure 2 and Figure 4B). The ability of the *bps1* extracts to evoke both a reduction in *pCYCB1;1::GUS* staining and the loss of starch granules supports the hypothesis that the hydrophilic extract contained the *bps* signal. Moreover, that changes in *pCYCB1;1::GUS* staining occurred more rapidly than loss of columella starch granules or QC46 expression suggests that loss of columella cell identity and QC46 expression in *bps1* mutants are indirect effects.

Bioassay Optimization

The initial tests of *bps1* extracts on roots relied on a 17-h incubation, which was selected for convenience. We tested shorter incubation times by comparing GUS-stained cells in the root meristems after 7, 12, and 17-h incubations (Figure 5A). Roots treated with wild-type extracts showed similar numbers of *pCYCB1;1::GUS*-stained cells, regardless of incubation time, indicating that wild-type extracts did not contain any general *pCYCB1;1::GUS* inhibitors. The wild-type roots incubated with *bps1* extracts showed a significant decrease in *pCYCB1;1::GUS*-stained cell numbers after 12 or 17-h incubations, but not after 7 h. This indicates that the *bps* signal requires more than 7 h to robustly and significantly affect root cell division. Because the 17-h incubation gave a robust response and was convenient, we retained this as our default incubation time.

Next we analyzed the amount of extract required to reduce cell division in wild-type roots. Extracts were typically isolated from 50 mg fresh weight of 7-day-old seedlings (~110 *bps1* and 30 wild-type seedlings). The polar extract was dried, re-suspended in 50–100 µl water (1.0–0.5 mg fresh weight µl^{-1}), and supplied in 30-µl aliquots to each microtiter dish well. We compared a dilution series of wild-type (L. er) and *bps1-1* extracts (1.0–0.01 mg µl^{-1})

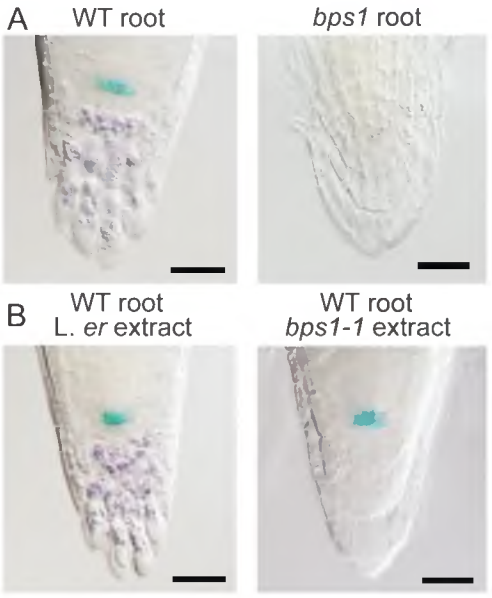

Figure 4. The *bps* Signal in Crude Extract Disrupts the Columella Cells in Wild-Type (WT) Roots.
(A) Five-day-old WT and *bps1* with QC:46::GUS marker, GUS and lugol-stained.
(B) GUS and lugol-stained WT roots, with QC:46::GUS marker, treated with WT or *bps1* extracts. Size bars: 50 µm.

(Figure 5B). In these experiments, we observed normal numbers of *pCYCB1;1::GUS*-stained cells in the root meristems of seedlings treated with wild-type extracts, regardless of concentration, again confirming the absence of any general inhibitors of *pCYCB1;1::GUS* expression in these tissue extracts. Extracts from *bps1-1* mutants showed activity when supplied in crude extracts, but only concentrations of 1.0 and 0.5 mg fresh weight µl^{-1} were robust and significant. Accordingly, the remaining experiments used 0.5 mg µl^{-1} extract concentrations, isolated from *bps1-1*.

Partial Chemical Characterization Suggests that the *bps* Signal Is a Metabolite

Signaling molecules can be generally classified as peptides, RNAs, or small molecules (including lipid derivatives and metabolites). As a step towards *bps* signal identification, we carried out some simple analyses to classify the compositional identity of the *bps* signal. First, we assessed its temperature stability. We found that wild-type and *bps1* extracts, boiled for 15 min, showed the same activity as their untreated controls (Figure 5C). This result indicated that the *bps* signal is heat-stable.

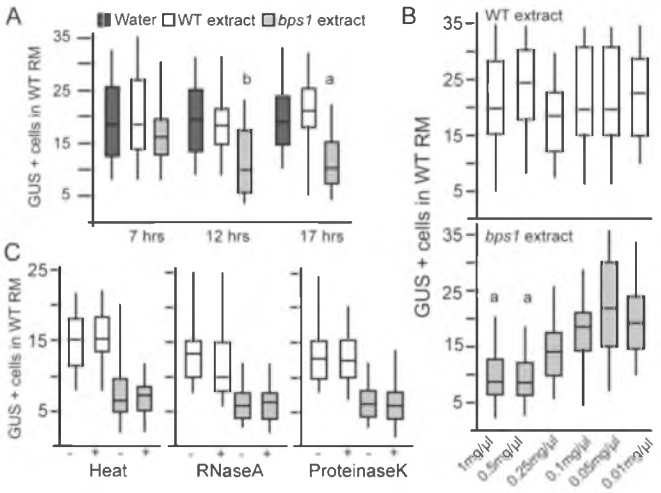

Figure 5. Partial Characterization of the *bps* Signal.
(A) The time-course sensitivity of the wild-type (WT) root meristem to the *bps* signal ($N = 14$ for each sample).
(B) WT (L.*er*) and *bps1-1* extracts were diluted to different strengths according to the fresh weight of the seedlings ($N = 12$ for each sample).
(C) Tests for sensitivity to heat, RNaseA and ProteinaseK of the *bps* signal ($N = 20$ for each sample). Results that are significantly different from the control samples are labeled with the letters a and b (Mann-Whitney U-test; a = $P < 0.005$ and b = $P < 0.05$).

Although heat stability might argue against the *bps* signal being a peptide, we also assessed whether it was sensitive to protease treatment. Aliquots of wild-type and *bps1* extracts were either incubated in Proteinase K (1 mg ml^{-1}, 2 h, 37°C), or incubated on ice without Proteinase K, and then tested for activity. We observed no effect of Proteinase K treatment on wild-type or *bps1* extracts (Figure 5C). Controls tested the Proteinase K activity by incubation with Bovine Serum Albumin (BSA), analyzed by SDS–PAGE, and found the Proteinase K to be highly activity (data not shown), making it unlikely that the *bps* signal is a peptide/protein.

Finally, we tested whether the *bps* signal showed sensitivity to RNaseA treatment. Aliquots of wild-type and *bps1* extracts were incubated in RNaseA (1 mg ml^{-1}, 37°C, 2 h). RNaseA treatment did not affect activity of either the wild-type or *bps1* extracts (Figure 5C). Controls tested the RNaseA activity by incubation with *Arabidopsis* RNA samples, analyzed by agarose gel, and found the RNaseA to be highly active (data not shown); thus, it is unlikely that the *bps* signal is an RNA molecule. Taken together with the Proteinase K result, these findings suggest that the *bps* signal is a small molecule, likely a metabolite.

General Considerations of Bioassay Development

Development of a bioassay is a critical step towards biochemical identification of novel signaling molecules. Recently, a petiole-feeding bioassay was developed to monitor SDI, shoot-derived inhibitor, which regulates root nodulation in legumes (Lin et al., 2010). Like the *bps* signal, SDI is an unknown mobile signal. Both the SDI and *bps* signal bioassays are quantitative and sensitive, and both reflect the unknown signaling molecule's biological activity. For SDI, the bioassay follows suppression of root nodules, whereas, for the *bps* signal, which inhibits growth, the bioassay follows suppression of cell cycle activity using the *pCYCB1;1::GUS* reporter (Colón-Carmona et al., 1999).

This cell cycle reporter has been widely used to analyze patterns of growth (Donnelly et al., 1999; Disch et al., 2006). However, it has also been shown to be sensitive to gibberellins, brassinosteroids, cytokinin, miRNAs, and tyrosine sulfated peptides (Achard et al., 2009; Ruzicka et al., 2009; Matsuzaki et al., 2010; Rodriguez et al., 2010; González-García et al., 2011). This study extends this list to include the *bps* signal.

Because *pCYCB1;1::GUS* expression can respond to diverse signals, we carried out extensive tests to ensure our experiments were following the *bps* signal. We observed reduced *pCYCB1;1::GUS* expression whether the *bps* signal was supplied by grafting or as a crude polar metabolite extract. We also observed reduced *pCYCB1;1::GUS* expression for two different *bps1* alleles. Control extracts, that is extracts from two wild-type accessions and one stunted mutant, did not reduce *pCYCB1;1::GUS* expression. Finally, the same extracts that diminished *pCYCB1;1::GUS* expression also induced the loss of columella cell starch granules, which is another *bps1* phenotype. Together, these observations indicate that the bioassay does provide a readout for the *bps* signal.

Development of this *bps* signal bioassay now allows us to start characterizing this mobile molecule, possibly by further

sub-fractionation strategies of the obtained polar extracts. Characterized mobile signaling molecules include peptides, mRNAs, and metabolites, and our data strongly suggest that the *bps* signal is a small metabolite. This assumption is based on the observation that the *bps* signal is resistant to RNase, protease, and heat, excluding the possibility that it is either a polypeptide or an RNA. These properties are similar to those of SDI, where the root nodulation bioassay revealed SDI to be a heat-stable, RNase and Protease-resistant molecule of less than 1000 Da (Lin et al., 2010). Finding that the *bps* signal is likely to be a small metabolite is also consistent with either a direct or an indirect role for carotenoids in biosynthesis of the *bps* signal (Van Norman and Sieburth, 2007). Future work identifying this signal will be an important step forward. Knowing the *bps* signal's chemical identity might allow us then to identify not only conditions that lead to its synthesis in wild-type plants, but also to identify the pathway that determines when and how it is synthesized. Linking the synthesis of the *bps* signal in normal plants to particular treatments will then allow us to place this orphan signaling molecule into a broader biological context.

METHODS

Plant Growth

Plants were generally grown at 22°C in 24-h light in Conviron TC-30 growth chambers. Col-0 seeds carrying the *pCYCB1;1::GUS* marker (Colon-Carmona et al., 1999) were grown in 96-well microtiter plates (three or four seeds per well) for the bioassay. Each well contained 75 µl GM (0.5 MS salts (Caisson Labs), 0.5 g L^{-1} MES (Fisher Scientific), 1% sucrose, and 0.5% agar (MP Biomedical). Extracts were prepared from 7-day-old seedlings grown on GM, except containing 0.8% agar, and *bps1-1* and its wild-type, L. *er*, were used unless otherwise noted.

Growth Transmission of the *bps* Signal

Grafting was carried out using 4-day-old seedlings, with the graft union stabilized by small siliconized tubing collars (Turnbull et al., 2002). Agarose plugs that separated rootstock and scion were composed of 0.8% agarose (Fisher Scientific, Molecular Biology Grade) in sterile water. Molten agarose was drawn into sterile siliconized tubing (0.012-inch internal diameter silicon tubing, Helixmark Co.). Pieces approximately 1–1.5 mm long were cut, and wild-type (*pCYCB1;1::GUS*) and *bps1* seedlings were cut transversely across the hypocotyl. Shoot and root segments were inserted into opposite ends of the tubing and maintained on sterile GM (2% agar) for 24 h. Agarose blocks that separated scion and rootstocks were about 0.5 mm.

Graft Transmission of the Cytokinin

Grafting was carried out as described above, except the scions were transgenic seedlings carrying the *pARR5:GUS* transgene. Positive controls were no-root transient micrografts where the agarose inside the siliconized tubing collars contained cytokinin, left in place for 24 h. Concentrations tested ranged from 1 µM to 1 mM, and both kinetin and 6-Benzylaminopurine (Caisson Labs) induced a robust response. These positive controls were compared to transient micrografts using wild-type and *bps1* roots, as described above.

GUS and Lugol Staining

GUS staining followed previously published protocols (Sieburth and Meyerowitz, 1997) except 3 mM X-Gluc concentration and 3-h incubations (37°C) were used. Seedlings were cleared and mounted with 70% chloral hydrate solution. Counts of the blue-stained cells were carried out using an Olympus BX-50 compound microscope and visualized under 400× magnification. To visualize starch granules in the root apex, lugol staining was carried out as described (Tsai et al., 2009). Following staining, tissue was rinsed (water) and mounted in saturated chloral hydrate. Observations of the treated tissue were carried out using an Olympus BX-50 microscope and images were captured with differential interference contrast optics on an Olympus BX-50 microscope.

Biochemical Analysis of Seedling Extracts

Extracts were prepared from 7-day-old seedlings that had been collected in 50-mg aliquots and flash-frozen in liquid nitrogen. We prepared crude methanol-chloroform-water extracts (Giavalisco et al., 2008), which were dried in a speed-vac (Labconco) and were re-suspended in sterile de-ionized water (typically 100 µl).

To determine whether the *bps* signal was sensitive to RNase or Protease, crude extracts from the wild-type and *bps1* were incubated in RNase A (1 mg ml^{-1}, 37°C, 2 h) and Proteinase K (1 mg ml^{-1}, 37°C, 2 h), respectively. Controls included RNaseA treatment of plant total RNA and Proteinase K treatment of Bovine Serum Albumen, followed by gel analyses. Tests for heat stability were carried out by incubating extract in a microfuge tube placed in a boiling water bath for 15 min. The treated extracts were then used in the bioassay, and the *bps* signal activity was compared to wild-type controls.

Statistical Analysis

We used the Mann-Whitney U-test to test the statistical significance of numbers of *pCYCB1;1::GUS*-stained cells following various treatments. This method was selected because the data are not normally distributed (Supplemental Figure 1). In this method, a two-tailed probability measure was used for all the data analyzed; statistical significance was determined at *P*-value of <0.05 or <0.005.

Expression Analysis

Transcript levels were measured using qRT–PCR, with three biological and two technical replicates. Total RNA extracted from 7-day-old seedlings (Qiagen RNeasy Mini Kit) was converted

to cDNA using Reverse Transcription System (Promega) following the standard protocol. Real-time RT–PCR was carried out using three biological replicates and two technical replicates. Reactions used 5 µl cDNA mixed with 20 µl of SYBR green reaction mixture (Fermentas), and run with the Mastercycler realplex EP (Eppendorf). Melt temperature, standard curve, and product sizes were verified for all reactions.

Four genes were compared for the internal reference (Actin2, GAPDH, At2g28390, and At1g13320) (Zhang et al., 2010) and At1g13320 was selected, as its expression was the most stable among the samples. The expression of each gene was calculated relative to the expression of internal control (At1g13320) and normalized to respective expression level in wild-type. Primer sequences are provided in Supplemental Table 1.

SUPPLEMENTARY DATA

Supplementary Data are available at *Molecular Plant Online*.

FUNDING

This work was supported by an award from CREES/NIFA to L.E.S. (2008–35304–04488).

ACKNOWLEDGMENTS

We thank Peter Gresshoff for advice during an early phase of this research, and Lothar Willmitzer and members of the Sieburth and Giavalisco research groups for useful discussions. We also thank John Cupp and Weiping Zhang for help with Proteinase K and RNase A controls, respectively. No conflict of interest declared.

REFERENCES

Achard, P., Gusti, A., Cheminant, S., Alioua, M., Dhondt, S., Coppens, F., Beemster, G.T.S., and Genschik, P. (2009). Gibberellin signaling controls cell proliferation rate in *Arabidopsis*. Curr. Biol. **19**, 1188–1193.

Aloni, R., Langhans, M., Aloni, E., Dreieicher, E., and Ullrich, C.I. (2005). Root-synthesized cytokinin in *Arabidopsis* is distributed in the shoot by the transpiration stream. J. Exp. Bot. **56**, 1535–1544.

Anastasiou, E., Kenz, S., Gerstung, M., MacLean, D., Timmer, J., Fleck, C. and Lenhard, M. (2007). Control of plant organ size by KLUH/CYP78A5-dependent intercellular signaling. Developmental Cell. **13**, 843–856.

Bennett, T., Sieberer, T., Willett, B., Booker, J., Luschnig, C., and Leyser, O. (2006). The *Arabidopsis* MAX pathway controls shoot branching by regulating auxin transport. Curr. Biol. **16**, 553–563.

Blilou, I., Xu, J., Wildwater, M., Willemsen, V., Paponov, I., Friml, J., Heidstra, R., Aida, M., Palme, K., and Scheres, B. (2005). The PIN auxin efflux facilitator network controls growth and patterning in *Arabidopsis* roots. Nature. **433**, 39–44.

Booker, J., Sieberer, T., Wright, W., Williamson, L., Willett, B., Stirnberg, P., Turnbull, C., Srinivasan, M., Goddard, P., and Leyser, O. (2005). MAX1 encodes a cytochrome P450 family member that acts downstream of MAX3/4 to produce a carotenoid-derived branch-inhibiting hormone. Developmental Cell. **8**, 443–449.

Boudolf, V., Vlieghe, K., Beemster, G.T.S., Magyar, Z., Acosta, J.A.T., Maes, S., Van Der Schueren, E., Inzé, D., and De Veylder, L. (2004). The plant-specific cyclin-dependent kinase CDKB1;1 and transcription factor E2Fa-DPa control the balance of mitotically dividing and endoreduplicating cells in *Arabidopsis*. Plant Cell. **16**, 2683–2692.

Colon–Carmona, A., You, R., Haimovitch–Gal, T., and Doerner, P. (1999). Technical advance: spatio-temporal analysis of mitotic activity with a labile cyclin–GUS fusion protein. Plant J. **20**, 503–508.

D'Agostino, I.B., Deruère, J., and Kieber, J.J. (2000). Characterization of the response of the *Arabidopsis* response regulator gene family to cytokinin. Plant Physiol. **124**, 1706–1717.

Davies, W., and Zhang, J. (1991). Root signals and the regulation of growth and development of plants in drying soil. Ann. Rev. Plant Biol. **42**, 55–76.

Delves, A.C., Mathews, A., Day, D.A., Carter, A.S., Carroll, B.J., and Gresshoff, P.M. (1986). Regulation of the soybean–Rhizobium nodule symbiosis by shoot and root factors. Plant Physiol. **82**, 588–590.

Dhondt, S., Coppens, F., De Winter, F., Swarup, K., Merks, R.M.H., Inze, D., Bennett, M.J., and Beemster, G.T.S. (2010). SHORT-ROOT and SCARECROW regulate leaf growth in *Arabidopsis* by stimulating S-phase progression of the cell cycle. Plant Physiol. **154**, 1183–1195.

Disch, S., Anastasiou, E., Sharma, V.K., Laux, T., Fletcher, J.C., and Lenhard, M. (2006). The E3 ubiquitin ligase BIG BROTHER controls *Arabidopsis* organ size in a dosage-dependent manner. Curr. Biol. **16**, 272–279.

Dolan, L., Janmaat, K., Willemsen, V., Linstead, P., Poethig, S., Roberts, K., and Scheres, B. (1993). Cellular organisation of the *Arabidopsis thaliana* root. Development. **119**, 71–84.

Donnelly, P.M., Bonetta, D., Tsukaya, H., Dengler, R.E., and Dengler, N.G. (1999). Cell cycling and cell enlargement in developing leaves of *Arabidopsis*. Developmental Biol. **215**, 407–419.

Dubrovsky, J.G., Sauer, M., Napsucialy-Mendivil, S., Ivanchenko, M.G., Friml, J., Shishkova, S., Celenza, J., and Benková, E. (2008). Auxin acts as a local morphogenetic trigger to specify lateral root founder cells. Proc. Natl Acad. Sci. U S A. **105**, 8790–8794.

Eriksson, S., Stransfeld, L., Adamski, N.M., Breuninger, H., and Lenhard, M. (2010). KLUH/CYP78A5-dependent growth signaling coordinates floral organ growth in *Arabidopsis*. Curr. Biol. **20**, 527–532.

Ferreira, P.C., Hemerly, A.S., Engler, J.D., Van Montagu, M., Engler, G., and Inzé, D. (1994). Developmental expression of the *Arabidopsis* cyclin gene cyc1At. Plant Cell. **6**, 1763–1774.

Flaishman, M.A., Loginovsky, K., Golobowich, S., and Lev–Yadun, S. (2008). *Arabidopsis thaliana* as a model system for graft union development in homografts and heterografts. J. Plant Growth Regul. **27**, 231–239.

Furutani, M., Vernoux, T., Traas, J., Kato, T., Tasaka, M., and Aida, M. (2004). PIN-FORMED1 and PINOID regulate boundary formation and cotyledon development in *Arabidopsis* embryogenesis. Development. **131**, 5021–5030.

Galinha, C., Hofhuis, H., Luijten, M., Willemsen, V., Blilou, I., Heidstra, R., and Scheres, B. (2007). PLETHORA proteins as dose-dependent master regulators of *Arabidopsis* root development. Nature. **449**, 1053–1057.

Giavalisco, P., Hummel, J., Lisec, J., Inostroza, A.C., Catchpole, G., and Willmitzer, L. (2008). High-resolution direct infusion-based mass spectrometry in combination with whole (13)c metabolome isotope labeling allows unambiguous assignment of chemical sum formulas. Anal. Chem. **80**, 9417–9425.

Goeres, D.C., Van Norman, J.M., Zhang, W., Fauver, N.A., Spencer, M.L., and Sieburth, L.E. (2007). Components of the *Arabidopsis* mRNA decapping complex are required for early seedling development. Plant Cell. **19**, 1549–1564.

Gomez-Roldan, V., Fermas, S., Brewer, P.B., Puech-Pagès, V., Dun, E.A., Pillot, J.-P., Letisse, F., Matusova, R., Danoun, S., Portais, J.-C. et al. (2008). Strigolactone inhibition of shoot branching. Nature. **455**, 189–194.

Gonzalez-Garcia, M.P., Vilarrasa-Blasi, J., Zhiponova, M., Divol, F. Mora-Garcia, S., Russinova, E. and Cano-Delgado, A.I. (2011). Brassinosteroids control meristem size by promoting cell cycle progression in *Arabidopsis* roots. Development. **138**, 849–859.

Gowing, D.J.G., Davies, W.J., and Jones, H.G. (1990). A positive root-sourced signal as an indicator of soil drying in apple, *Malus x domestica Borkh*. J. Exp. Bot. **41**, 1535–1540.

Hemerly, A., Bergounioux, C., Van Montagu, M., Inze, D., and Ferreira, P. (1992). Genes regulating the plant cell cycle: isolation of a mitotic-like cyclin from *Arabidopsis thaliana*. Proc. Natl Acad. Sci. U S A. **89**, 3295–3299.

Lee, D.-K., Van Norman, J.M., Murphy, C., Adhikari, E., Reed, J.W., and Sieburth, L.E. (2012). In the absence of BYPASS1-related gene function, the bps signal disrupts embryogenesis by an auxin-independent mechanism. Development. **139**, 805–815.

Lin, Y.-H., Ferguson, B.J., Kereszt, A., and Gresshoff, P.M. (2010). Suppression of hypernodulation in soybean by a leaf-extracted, NARK- and Nod factor-dependent, low molecular mass fraction. New Phytol. **185**, 1074–1086.

Liu, J., Mehdi, S., Topping, J., Tarkowski, P., and Lindsey, K. (2010). Modelling and experimental analysis of hormonal crosstalk in *Arabidopsis*. Molecular Systems Biology. **6**, 373.

Matsuzaki, Y., Ogawa-Ohnishi, M., Mori, A., and Matsubayashi, Y. (2010). Secreted peptide signals required for maintenance of root stem cell niche in *Arabidopsis*. Science. **329**, 1065–1067.

Menges, M., De Jager, S.M., Gruissem, W., and Murray, J.A.H. (2005). Global analysis of the core cell cycle regulators of *Arabidopsis* identifies novel genes, reveals multiple and highly specific profiles of expression and provides a coherent model for plant cell cycle control. Plant J. **41**, 546–566.

Moore, R. (1984). A model for graft compatibility–incompatibility in higher plants. Am. J. Bot. **71**, 752–758.

Müller, R., Borghi, L., Kwiatkowska, D., Laufs, P., and Simon, R. (2006). Dynamic and compensatory responses of *Arabidopsis* shoot and floral meristems to CLV3 signaling. Plant Cell. **18**, 1188–1198.

Naseem, M., Philippi, N., Hussain, A., Wangorsch, G., Ahmed, N., and Dandekar, T. (2012). Integrated systems view on networking by hormones in *Arabidopsis* immunity reveals multiple crosstalk for cytokinin. Plant Cell. **24**, 1793-1814.

Potuschak, T., and Doerner, P. (2001). Cell cycle controls: genome-wide analysis in *Arabidopsis*. Curr. Opin. Plant Biol. **4**, 501–506.

Riou-Khamlichi, C., Huntley, R., Jacqmard, A., and Murray, J.A. (1999). Cytokinin activation of *Arabidopsis* cell division through a D-type cyclin. Science. **283**, 1541–1544.

Rodriguez, R.E., Mecchia, M.A., Debernardi, J.M., Schommer, C., Weigel, D., and Palatnik, J.F. (2010). Control of cell proliferation in *Arabidopsis thaliana* by microRNA miR396. Development. **137**, 103–112.

Rojo, E., Sharma, V.K., Kovaleva, V., Raikhel, N.V., and Fletcher, J.C. (2002). CLV3 is localized to the extracellular space, where it activates the *Arabidopsis* CLAVATA stem cell signaling pathway. Plant Cell. **14**, 969–977.

Ruzicka, K., Simásková, M., Duclercq, J., Petrásek, J., Zazimalová, E., Simon, S., Friml, J., Van Montagu, M.C.E., and Benková, E. (2009). Cytokinin regulates root meristem activity via modulation of the polar auxin transport. Proc. Natl Acad. Sci. U S A. **106**, 4284–4289

Sabatini, S., Beis, D., Wolkenfelt, H., Murfett, J., Guilfoyle, T., Malamy, J., Benfey, P., Leyser, O., Bechtold, N., Weisbeek, P., et al. (1999). An auxin-dependent distal organizer of pattern and polarity in the *Arabidopsis* root. Cell. **99**, 463–472.

Schoof, H., Lenhard, M., Haecker, A., Mayer, K.F., Jürgens, G., and Laux, T. (2000). The stem cell population of *Arabidopsis* shoot meristems in maintained by a regulatory loop between the CLAVATA and WUSCHEL genes. Cell. **100**, 635–644.

Segers, G., Gadisseur, I., Bergounioux, C., de Almeida Engler, J., Jacqmard, A., Van Montagu, M., and Inzé, D. (1996). The *Arabidopsis* cyclin-dependent kinase gene cdc2bAt is preferentially expressed during S and G2 phases of the cell cycle. Plant J. **10**, 601–612.

Sieburth, L.E., and Meyerowitz, E.M. (1997). Molecular dissection of the AGAMOUS control region shows that *cis* elements for spatial regulation are located intragenically. Plant Cell. **9**, 355–365.

Sorefan, K., Booker, J., Haurogné, K., Goussot, M., Bainbridge, K., Foo, E., Chatfield, S., Ward, S., Beveridge, C., Rameau, C., et al. (2003). MAX4 and RMS1 are orthologous dioxygenase-like genes that regulate shoot branching in *Arabidopsis* and pea. Genes Dev. **17**, 1469–1474.

Tsai, H.-L., Lue, W.-L., Lu, K.-J., Hsieh, M.-H., Wang, S.-M., and Chen, J. (2009). Starch synthesis in *Arabidopsis* is achieved by spatial cotranscription of core starch metabolism genes. Plant Physiol. **151**, 1582–1595.

Turnbull, C.G.N., Booker, J.P., and Leyser, H.M.O. (2002). Micrografting techniques for testing long-distance signalling in *Arabidopsis*. Plant J. **32**, 255–262.

Umehara, M., Hanada, A., Yoshida, S., Akiyama, K., Arite, T., Takeda-Kamiya, N., Magome, H., Kamiya,Y., Shirasu, K., Yoneyama,K., et al. (2008). Inhibition of shoot branching by new terpenoid plant hormones. Nature. **455**, 195–200.

Van Norman, J.M., and Sieburth, L.E. (2007). Dissecting the biosynthetic pathway for the bypass1 root-derived signal. Plant J. **49**, 619–628.

Van Norman, J.M., Frederick, R.L., and Sieburth, L.E. (2004). BYPASS1 negatively regulates a root-derived signal that controls plant architecture. Curr. Biol. **14**, 1739–1746.

Van Norman, J.M., Murphy, C., and Sieburth, L.E. (2011). BYPASS1: synthesis of the mobile root-derived signal requires active root growth and arrests early leaf development. BMC Plant Biol. **11**, 28.

Vercruyssen, L., Gonzalez, N., Werner, T., Schmülling, T., and Inzé, D. (2011). Combining enhanced root and shoot growth reveals cross talk between pathways that control plant organ size in *Arabidopsis*. Plant Physiol. **155**, 1339–1352.

Wang, Y.K.R. (1996). Vascular differentiation in the graft union of in-vitro grafts with different compatibility: structural and functional aspects. J. Plant Physiol. **147**, 521–533.

Yadav, R.K., Perales, M., Gruel, J., Girke, T., Jönsson, H., and Reddy, G.V. (2011). WUSCHEL protein movement mediates stem cell homeostasis in the *Arabidopsis* shoot apex. Genes Dev. **25**, 2025–2030.

Yin, H., Yan, B., Sun, J., Jia, P. Zhang, Z., Yan, X., Chai, J., Ren, Z., Zheng, G., and Liu, H. (2012). Graft-union development: a delicate process that involves cell–cell communication between scion and stock for local auxin accumulation. J. Exp. Bot. **63**, 4219–4232.

Zhang, W., Murphy, C., and Sieburth, L.E. (2010). Conserved RNaseII domain protein functions in cytoplasmic mRNA decay and suppresses *Arabidopsis* decapping mutant phenotypes. Proc. Natl Acad. Sci. U S A. **107**, 15981–15985.

CHAPTER 3

GENETIC AND INHIBITOR APPROACHES TO IDENTIFYING THE *bps* SIGNAL'S BIOSYNTHETIC PATHWAY

3.1 Abstract

To characterize the biosynthetic pathway for the *bypass* (*bps*) signal, a metabolite that is overproduced in roots of the *Arabidopsis bypass1* (*bps1*) mutant, we used both chemical inhibitors and mutants to block select metabolic pathways. Because the *bps* signal causes severe shoot and root growth defects, the severity of the *bps1* phenotype provided a simple method to assess *bps* signal synthesis. Levels of the *bps* signal were confirmed in selected genotypes/conditions using our bioassay[44]. Here we show that *bps1* mutants are resistant to an analog of tryptophan (Trp), 5-methyl tryptophan (5-MT), suggesting that there is high Trp flux in *bps1* mutants. When Trp biosynthesis is limited in *bps1* mutants (through double mutants with *trp2* and *trp3* biosynthetic mutants), leaf development was partially rescued. The rescued phenotype is restored to *bps1* when *trp2 bps1* double mutants are grown on media containing Trp, and the bioassay also shows that *trp2 bps1* double mutants have a reduced level of *bps* signal activity. These experiments suggest that Trp might be the biosynthetic precursor to the *bps* signal. One of the major products that are derived from Trp is the glucosinolates. Further genetic analyses eliminated glucosinolates as a *bps* signal precursor. These analyses provide very useful starting material for chemical fractionation in our search for the elusive *bps* signal. Knowing the chemical identity of this mobile compound is of strong interest because it would allow us to test whether normal plants produce it, as would be expected if it is a plant hormone.

3.2 Introduction

The *Arabidopsis bps1* mutant overproduces a compound, the *bps* signal, in its roots that acts locally to cause abnormal root development, and also functions long distance to cause the arrest of shoot growth. My main goal is to characterize the biosynthetic pathway of this compound and identify it chemically. My approach to characterize this compound's biosynthetic pathway is to identify inhibitors that disrupt its synthesis or mutants with defects in biosynthesis. Previous work using inhibitors showed that the herbicide fluridone partially rescued the *bps1* mutant phenotype[40,45]. Fluridone inhibits phytoene desaturase, which catalyzes an early step of carotenoid biosynthesis[46]. This observation supported a carotenoid origin for the *bps1* root-derived signal. However, biochemical comparisons of carotenoid profiles failed to find support for carotenoids as the *bps* signal precursor (Sieburth, personal communication). An alternative interpretation of the carotenoid biosynthetic inhibitor experiments is that *bps1* phenotypic rescue was due to plastid photooxidation, a consequence of carotenoid loss, not the loss of carotenoids themselves. Photooxidation would eliminate plastids, even plastids in the roots, and thus any biosynthetic pathway with a step that localized to plastids would be lost. Among the many pathways that have essential biosynthetic steps that are catalyzed in plastids, our studies implicated Tryptophan (Trp) as a strong candidate for the *bps* signal precursor.

3.2.1 Tryptophan biosynthesis and metabolism

Trp is an essential amino acid and it serves as a building block for protein synthesis in all organisms. Apart from protein synthesis, Trp is used as a precursor for diverse compounds. For example, in animals, Trp is a precursor for the neurohormone serotonin and the vitamin nicotinic acid. In plants, Trp is the precursor for the synthesis of the phytohormone auxin. In the Brassicales, it is also used for the synthesis of the antimicrobial phytoalexins, glucosinolates, and both indole- and anthranilate-derived alkaloids[47,48].

The biosynthetic pathways of Trp in both plants and microorganisms have been well elucidated and they exhibit many biochemical similarities. Seven different enzymatic steps lead to the synthesis of Trp from chorismate[47]: these are catalyzed by anthranilate synthase, which is composed of alpha and beta subunits (Fig. 3.1, step 1)[49,50]; phosphoribosylanthranilate transferase (Fig. 3.1, step 2)[51]; phosphoribosylanthranilate isomerase (Fig. 3.1, step 3)[52]; indole-3-glycerolphosphate synthase (Fig. 3.1, step 4)[53]; the Trp synthase alpha subunit (Fig. 3.1, step 5)[54] and the beta subunit (Fig. 3.1, step 6)[54].

TRP3 and *TRP2* genes encode TSA (the alpha subunit) and TSB (the beta subunit) of tryptophan synthase, respectively. *TRP3* is required for the conversion of indole-3-glycerol phosphate into indole and *TRP2* is required for the conversion of indole into tryptophan. The *trp3-2* allele contains a nonsense mutation in the *TSA* gene and the TSA protein level is less than 10% of the wild type[47]. The *trp2-1* allele is a recessive mutation in the *TSB* gene and it has reduced TSB subunit activity[55,56]. As might be expected when an essential

amino acid is present in limited quantities, the *trp3* and *trp2* mutants exhibit developmental defects under normal growth conditions, including being small, and having pale-green leaves with dark veins[47,57].

One of the major products that are derived from Trp is glucosinolates. Glucosinolates are naturally occurring glucosides, mainly produced in mustard, cabbage and horseradish, which contain sulfur and nitrogen. These natural chemicals are known to contribute to plant defense against herbivore and diseases. To date, more than 120 different glucosinolates are known to occur naturally in plants and they are categorized into aliphatic, aromatic, and indole glucosinolates. Indole glucosinolates (IGs) are produced from tryptophan. In *Arabidopsis*, IGs are produced from Trp by the enzymatic activity of two cytochrome P450 enzymes encoded by CYP79B2 and CYP79B3. CYP79B2 and CYP79B3 convert Trp to IAOx; IAOx can be converted to both IAA and IG[58,59]. CYP79B2 and CYP79B3 are functionally redundant; neither of the single mutants, *cyp79B2* and *cyp79B3*, have visible phenotypes. However, *cyp79B2 cyp79B3* double mutants have short hypocotyls, a smaller stature, and strongly reduced IG levels, suggesting that both CYP79B2 and CYP79B3 contribute to IG production[60].

3.2.2 Amino acid analogs

Amino acid analogs are compounds that appear similar to amino acids structurally, and can be recognized by the translational machinery as the similar amino acid, but they do not have the same structure. This structural difference means that proteins incorporating the analog are unlikely to fold correctly, and

thus often are unable to perform their functions. For example, enzymes synthesized with analogs might lack activity[61]. For this reason, most organisms are highly sensitive to supplied amino acid analogs. However, organisms have developed ways to resist the toxic effects of amino acid analogs. First, resistant cells might degrade the analog. Alternatively, resistant cells might alter the regulation of the pathway, leading to the overproduction of the amino acid effectively diluting the analog. Finally, resistance to amino acid analogs might occur if the analog is used in an alternative biochemical pathway, again essentially diluting the concentration of the analog[62].

Example of resistance to analog due to the overproduction of endogenous amino acid comes from an *Arabidopsis* mutant, *amt-1*. Endogenous Trp is over-produced in *amt-1* mutants and the overproduction is associated to *amt-1* being resistance to α-methyltryptophan (αMT), an analog of Trp. *amt-1* is a dominant mutant with a point mutation in *ASA1* gene, and it has higher anthranilate synthase (AS) activity. *ASA1* encodes the α subunit of AS and AS converts chorismate to anthranilate, the first step in the Trp biosynthesis pathway (Fig. 3.1). Due to the higher AS activity, Trp is up-regulated in these mutants. An interpretation of *amt-1* resistance to αMT was linked to the overproduction of the amino acid, which diluted the toxic effect of αMT[63,64].

Example of resistance where there is high flux of the amino acid analog comes from *yucca* mutants and plants overexpressing *CYP79B2*. CYP79B2 is an enzyme in the first committed step of IG production from Trp. *yucca* mutants and seedlings overexpressing *CYP79B2* are resistant to 5-MT, an analog of Trp.

The resistance of *yucca* mutants to 5-MT is connected to auxin being overproduced in these mutants. Trp is the biosynthetic precursor to auxin and 5-mT is less toxic to *yucca* mutants because it is removed from the Trp pool. 5-MT is converted to 5-methyl IAA, which is an active auxin[65]. In *Arabidopsis* seedlings, overexpressing *CYP79B2* the concentration of Trp is decreased because the conversion of Trp to IAOx is increased[58].

Yet another example of resistance to amino acid analogs comes from *trp2-1* mutants. *trp2-1* mutants are insensitive to the toxic effects of 5-fluoroindole, an analog of Trp. *trp2-1* mutant is deficient in TSB subunit activity (Fig. 3.1). This result suggests that the toxicity is due to the conversion of 5-fluroindole to 5-flurotryptophan by wild type TSB protein[66].

Here, we address the possibility that Trp might be the biosynthetic precursor to the *bps* signal by carrying out experiments using amino acid analogs and genetic approaches.

3.3 Materials and methods

3.3.1 Growth conditions and plant materials

Plants were grown at 22^0C in 24-hours light, in a Conviron TC-30 growth chamber, on petri-plates containing plant growth medium (GM). GM consists of 0.5X Murashige and Skoog salts (Cassion labs), 0.5 g L^{-1} MES (Fisher Scientific), 1% sucrose, and 0.8 % agar (MP Biomedical, LLC). Seeds were imbibed in the dark at 4^0 C for 2 days prior to transfer to growth rooms.

Two *bps1* mutant alleles were used for the experiments: *bypass1-2* (*bps1-2)* is an insertion allele in Columbia-0 (Col-0) accession, and *bypass1-1* (*bps1-1)*

is an EMS-generated allele that was isolated in the *Landsberg erecta* (L *.er*) accession[40]. *trp2-1* and *cyp79B2 cyp79B3* were used to generate double and triple mutants with *bps1-2*. 7 dpi (days post imbibition) *bps1-1*, *bps1-2*, *trp2-1 bps1-2*, *cyp79B2 cyp79B3 bps1-2* and their respective wild type seedlings were used for phenotypic assessment as well as metabolite extraction for the bioassay.

3.3.2 Amino acid and amino acid analogs treatments

Wild type and *bps1* seedlings were grown on GM containing 5-MT (Sigma-Aldrich) and L-canavanine (an analog of arginine)[67] (Sigma-Aldrich) at 0, 25, 50, 75, and 100 µM concentrations and DL-4-flurophenylalanine (an analog of phenylalanine)[68] (Sigma-Aldrich) at 0, 40, 80, 120, and 160 µM concentrations. The seedlings were grown at 22^0 C, 24-hours day light and the phenotypes were examined at 7 dpi. For Trp supplement experiments, *trp2-1 bps1-2*, *bps1-2*, *trp2-1,* and Col were grown on GM containing 250 µM Trp (Sigma-Aldrich). Phenotypic assessment of seedlings grown on the Trp media was done at 12 dpi.

3.3.3 Construction of double and triple mutants,
and genetic analysis

Double and triple mutants that combined *bps1-2* with *trp2-1, trp3-1*, or *cyp79B2 cyp79B3* were generated using standard approaches. To make the genetic background consistent (all Col-0), the *bps1-2* allele was used for all the crosses. We crossed heterozygous *bps1-2* with homozygous *trp2-1, trp3-1*, or *cyp79B2 cyp79B3* lines. All seedlings in the F1 generation were heterozygous

for *trp2-1* or *trp3-1* and they were either wild type (WT) or heterozygous for *bps1*. F1 generation plants were allowed to self-pollinate to generate F2 generation. Parents of the F2 generations that were heterozygous for both *trp2-1* or *trp3-1* and *bps1* were identified, by testing if the seeds segregated homozygous *trp2-1* or *trp3-1* and *bps1* mutants. F2 generations from the double heterozygous parents that were homozygous for *trp2* or *trp3* and heterozygous for *bps1* were identified. Lines homozygous for *trp2-1* or *trp3-1* were identified by analyzing the phenotype of the seedlings. Heterozygous *bps1* lines were identified by testing if the seeds segregated homozygous *bps1*.

To generate *cyp79B2 cyp79B3 bps1* triple mutants, heterozygous *bps1-2* was crossed to homozygous *cyp79B2 cyp79B3.* All seedlings in the F1 generation were heterozygous for *cyp79B2 cyp79B3* and they were either WT or heterozygous for *bps1*. F1 generation plants were allowed to self-pollinate to generate F2 generation. Parents of the F2 generations that were heterozygous for both *cyp79B2 cyp79B3* and *bps1* were identified. Lines that were heterozygous for *cyp79B2 cyp79B3* were analyzed by genotyping and heterozygous *bps1* were identified by testing if the seeds segregated homozygous *bps1* mutants. F2 generations from the double heterozygous parents that were homozygous for *cyp79B2 cyp79B3* and heterozygous for *bps1* were identified by approaches similar to that described above.

3.3.4 Analysis of the *bps* signal activity

The *bps* signal activity was quantified using the bioassay as described in Chapter 2[44]. 75µl of GM was placed in each well of a 96-well microtiter plate,

and three to five Col-0 seeds containing *pCYCB1;1::GUS* marker were sown on each well. Extracts were prepared from 7 dpi seedlings that had been collected in 50-mg aliquots and flash-frozen in liquid nitrogen. We prepared crude methanol-chloroform-water extracts, which were dried in a speed-vac (labconco) and were resuspended in water (120µl). 40µl of the extract was applied to each well of the microtiter plate; extracts from each genotype were applied to three wells and incubated for 17 hours. After 17 hours the seedlings were taken out of the microtiter plate and were GUS stained for 3 hours. GUS staining followed previously published protocols[69] except 3mM X-Gluc concentration and 3 hours incubation (37^0) were used. Seedlings were cleared and mounted with 70% chloral hydrate solutions. The number of GUS positive cells in the wild type root meristems were counted using an Olympus BX-50 compound microscope under 400X magnification.

3.4 Results

3.4.1 Amino acid analog-resistance suggests that *bps1* mutants have high Trp flux

A chance observation led us to test the response of *bps1* mutants to amino acid analogs. We grew *bps1* and wild type plants on media supplement with 5-methyl tryptophan (5-MT), an analogue of Trp. Both the *bps1-1* and *bps1-2* alleles showed similar responses. Wild type, both Col and L*. er*, which are sensitive to 5-MT, showed reduced hypocotyl length, shorter roots, and smaller cotyledons than the controls on the lowest concentration tested, 25 µM of 5-MT. At 50 µM and 75 µM of 5-MT, the roots were even shorter and the cotyledons

were much smaller. At the highest concentration tested, 100 μM, the seedlings germinated but did not develop cotyledons and leaves. This observation suggested that the wild type seedlings showed a dose-dependent sensitivity to 5-MT (Fig. 3.2A). However, at all concentrations tested, both the alleles *bps1-2* and *bps1-1* looked similar to *bps1* grown on control media (Fig. 3.2A). This observation indicated that *bps1* mutants were 5-MT resistant. To test if *bps1* seedlings were resistant to all amino acid analogs, or whether resistance was 5-MT specific, we grew *bps1* mutants on media containing L- canavanine or 4-fluorophenylalanine, analogs of arginine and phenylalanine, respectively. Wild type seedlings, both Col and L. *er*, showed a similar sensitive phenotype to L-canavanine as they showed to 5-MT, i.e., reduced hypocotyl length, shorter roots, and smaller cotyledons. Similar to wild type, both *bps1-2* and *bps1-1* alleles were also sensitive to all the concentrations tested. However, *bps1-1* was more sensitive to L-canavanine than *bps1-2* (Fig. 3.2B). Wild type seedlings, both Col and L. *er*, showed a similar response of sensitivity to 4-flurophenylalanine; however, the sensitivity was less severe than that to 5-MT or to L-canavanine (Fig. 3.2C). Similar to wild type, both *bps1-2* and *bps1-1* alleles showed a sensitive phenotype to all concentrations of 4-flurophenylalanine and L-canavanine. This suggests that resistance of *bps1* mutants is 5-MT-specific (Fig. 3.2C).

There are two general ways that resistance to amino acid analogs can occur. One way is the up-regulation of the production of the natural amino acid, which effectively dilutes the analog[61]. The other way is to deplete the analog,

e.g., by diluting the analog into an alternative pathway. Because we believe that *bps1* mutants overproduce the *bps* signal, it is attractive to hypothesize that resistance to 5-MT in *bps1* mutant results from the incorporation of 5-MT into the *bps* signal, suggesting that the natural precursor to the *bps* signal is Trp.

3.4.2 Limiting TRP biosynthesis partially suppresses the *bps1* phenotype and the amount of *bps* signal is reduced

We reasoned that if Trp is the precursor to the *bps* signal, then double mutants that reduced Trp biosynthesis might also limit the synthesis of the *bps* signal, and so result in a partially rescued phenotype. To test this possibility, we generated *bps1-2* double mutants with *trp2-1* and *trp3-1* mutants. The *trp3-1* mutant has a lesion in the Trp synthase α subunit and *trp2-1* has a mutation in the Trp synthase β subunit, and both have reduced Trp levels[47,54]. Homozygous *trp3-1* and *trp2-1* single mutants produce small leaves that are pale yellow in color (Fig. 3.3). *bps1* mutants develop small leaf primordia, with no trichomes, that arrest prior to leaf blade expansion[40] (Fig. 3.3). However, homozygous *trp2 bps1* and *trp3 bps1* double mutants produced broad well-developed leaves with trichomes, similar to that of wild type (Fig. 3.3). The chi-square value for the seedlings with *bps1*-like phenotype indicated that the partial rescue of these double mutants was statistically significant (Table 3.1).

The suppressed phenotype of *trp2 bps1* and *trp3 bps1* mutants might be due to reduced Trp levels. If this was the case, we hypothesized that if the double mutants are supplied with exogenous Trp, the phenotype will revert back to *bps1*-like. To test this possibility, we supplied Trp to *trp2 bps1* and *trp3 bps1*

double mutants by growing them in media containing Trp. When *trp2 bps1* and *trp3 bps1* mutants were grown on regular media, they developed well-developed leaves with trichomes, whereas *bps1* single mutants produced small, radialized leaves without trichomes when grown on regular media. When *trp2 bps1* and *trp3 bps1* double mutants were grown on media containing 250 μM Trp, they showed a phenotype similar to *bps1* single mutants (Fig. 3.3). This indicated that the *bps1*-like phenotype was reinstated when there is Trp availability, suggesting that the *bps* signal derived from Trp. These observations link TRP availability to production of the *bps* signal.

To test whether the *bps* signal was reduced in *trp2 bps1* double mutants, we quantified the *bps* signal in the double mutants using the bioassay. Extracts from negative controls, Col and *trp2,* showed a normal number of dividing cells in WT root meristem. Extracts from positive control, *bps1-2,* showed a reduced number of dividing cells in the WT root meristem. *trp2 bps1* extracts showed a reduced number of dividing cells than the wild type extracts but higher number of dividing cells than the *bps1-2* extracts (Fig. 3.4). This result confirms that the *trp2 bps1* double mutants have a reduced level of the *bps* signal in comparison to *bps1* single mutant. Taken together, these data indicate that a supply of Trp is required for the production of *bps* signal, and suggest that Trp might be the biosynthetic precursor to *bps* signal.

3.4.3 *bps* signal is not indole glucosinolate or its derivative

Partial rescue of the *trp2 bps1* double mutant phenotype suggested that Trp is the biosynthetic precursor of the *bps* signal. One of the major sinks for Trp

in *Arabidopsis* is the production of indole glucosinolates (IG)[70]. It is possible that the *bps* signal is derived from the IG pathway. If this were the case, we predicted that if we blocked IG synthesis in the *bps1* mutants, the *bps1* mutant would show a rescued phenotype. To test this possibility, we generated triple mutants by combining *bps1-2* and *cyp79B2 cyp79B3* double mutants. *cyp79B2* and *cyp79B3* are the mutants of two cytochrome P450 enzymes, CYP79B2 and CYP79B3. These enzymes carry out the first step of the glucosinolate biosynthetic pathway, conversion of Trp into indole-3-acetaldoxime (IAOx)[58] (Fig. 3.1). The *bps1-2 cyp79B2 cyp79B3* triple mutants were indistinguishable from *bps1-2* single mutants (Fig. 3.5).

To confirm that the *bps* signal was still produced in these triple mutants, we quantified *bps* signal activity in the triple mutants using the bioassay. Extracts from controls, wild type (Col), and the *cyp79B2 cyp79B3* double mutant showed a normal number of dividing cells in the WT root meristem. Extracts from *cyp79B2 cyp79B3 bps1-2* triple mutants showed a reduced number of dividing cells similar to that of extracts from *bps1-2* single mutants (Fig. 3.4). This result implied that *bps1-2 cyp79B2 cyp79B3* triple mutants have a similar level of *bps* signal as the *bps1-2* single mutants. These results indicated that the *bps* signal is not derived from the glucosinolate pathway.

3.5 Discussion

Plants utilize long-distance signaling to communicate information from root to shoot or from shoot to root. One group of signaling molecules that plays a vital role in long-distance communication is small metabolites. The main goal of the

project described here is to identify the small metabolite that is overproduced in *Arabidopsis* mutant, *bps1*, and that causes growth arrest. *bps1* mutant roots produce a graft-transmissible signal, *bps* signal, that causes abnormal root development and shoot growth is arrested[40]. We want to know if the *bps* signal is a novel plant hormone. Identification of the *bps* signal might allow us to begin to understand whether normal plants produce it, at what conditions they produce it, and how BPS1 controls its production.

Previous work to identify the *bps* signal supported a carotenoid origin for the *bps* signal. Inhibitor of carotenoid biosynthesis, fluridone, partially rescued the *bps1* phenotype[45]. The simplest explanation of these results was that a carotenoid was the precursor to *bps* signal. However, biochemical comparisons of carotenoid profiles did not support carotenoid as the precursor to the *bps* signal[45]. An alternative interpretation for this result is that the partial rescue of the *bps1* mutants was due to the plastid photooxidation that is caused by the loss of the carotenoid. Plastid photooxidation eliminates plastids, thus any biosynthetic pathway with a step that is localized to plastids would be lost. A pathway that has essential biosynthetic steps that are catalyzed in plastids is Trp biosynthesis. Thus, we considered Trp as a good candidate for the *bps* signal biosynthesis pathway.

We tested for Trp as the biosynthetic precursor to the *bps* signal by using both analogs and genetic approaches. Using an analog approach, we showed that *bps1* mutants are resistant to 5-MT, an analog of Trp. The resistance of *bps1* mutants to amino acid analogs was specific to Trp; *bps1* mutants were as

sensitive as the wild type when they were grown on media containing 4-fluorophenylalanine or L- canavanine, analogs of phenylalanine and arginine, respectively. The toxicity of 5-MT to seedlings is due to 5-MT being incorporated into proteins in place of Trp so that the proteins produced do not fold properly or lose activity. However, cells can acquire resistance in two different ways. One way is that Trp might be overproduced, which will dilute the toxic effect of 5-MT. Alternatively, 5-MT might be fed into the production of a compound that uses Trp as its biosynthetic precursor. The reasonable explanation of the *bps1* mutants being 5-MT resistant is that the mutants have high flux of 5-MT into *bps* signal production. If this was the case, we reasoned that Trp might be the biosynthetic precursor to the *bps* signal. To test if Trp was the biosynthetic precursor to the *bps* signal, we used a genetic approach. We observed partial rescue of leaf development in *bps1* mutants when double mutants were generated between *bps1* and *trp2* or *trp3*, mutants in the Trp biosynthesis pathway. We further showed that the rescue of *bps1* leaf development in the double mutant was due to the reduced Trp level. When *trp2 bps1* or *trp3 bps1* double mutants were grown on media supplemented with Trp, the *bps1* like phenotype was restored. By using the *bps* signal bioassay, we showed that the metabolite extracts from *trp2 bps1* double mutants had a reduced level of *bps* signal. This finding correlated with the phenotypes of the *trp2 bps1* double mutant and suggested that the phenotypic rescue of *trp2 bps1* double mutant is due to the reduction of the *bps* signal production and the *bps* signal is Trp derivative.

Our big question is if Trp is the precursor to the *bps* signal, then what is the *bps* signal. The major product that is produced from Trp is indole glucosinolates. So, we tested if *bps* signal is derived from indole glucosinolates. When we generated *bps1* triple mutants with *cyp79B2 cyp79B3* double mutants, triple mutants were indistinguishable from *bps1* single mutants. The *cyp79B2 cyp79B3* mutants cannot catalyze the production of IAOx from Trp, which is required for the production of indole glucosinolates. We have shown that metabolite extracts from *cyp79B2 cyp79B3 bps1* triple mutants have a similar level of *bps* signal activity as the *bps1* single mutants. These results indicate that the *bps* signal is not indole glucosinolate or its derivative.

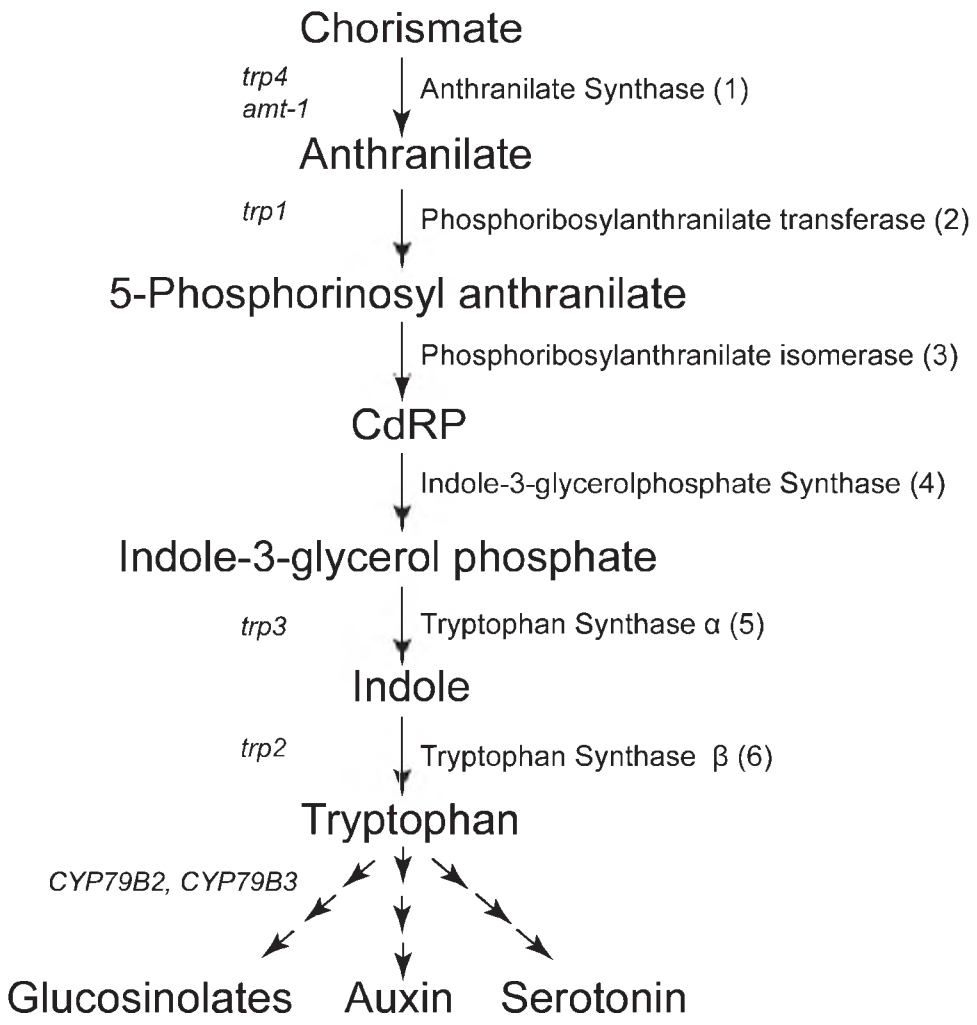

Figure 3.1: The tryptophan biosynthesis and metabolism pathway. Genes with mutations are shown on the left, and enzyme names and step numbers (in parentheses) on the right; ➔➔➔means >1 steps. CdRP = 1-(O-carboxyphenylamino)-1-deoxyribulose-5-phosphate. Figure modified from (Radwanski & Last, 1995).

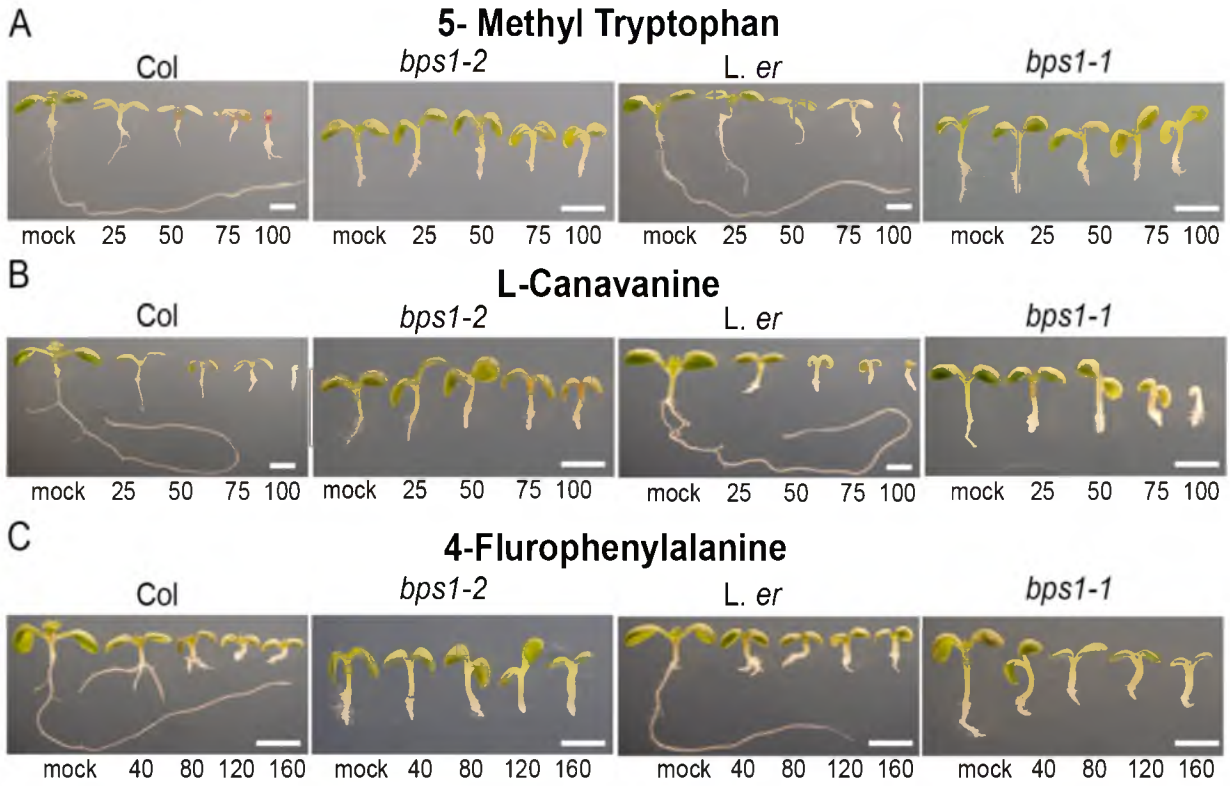

Figure 3.2: Seedling phenotype of wild type and *bps1* mutants grown on media containing amino acid analogs. Depicted here are 7 dpi (days post imbibition) seedlings. Col and L *.er* are sensitive to 5-MT (A), L-Canavanine (B), and 4-Flurophenylalanine (C). *bps1-2* and *bps1-1* are resistant to 5-MT (A) but are sensitive to L-Canavanine (B) and 4-Flurophenylalanine (C) at all the concentrations tested. Size bars = 2mm.

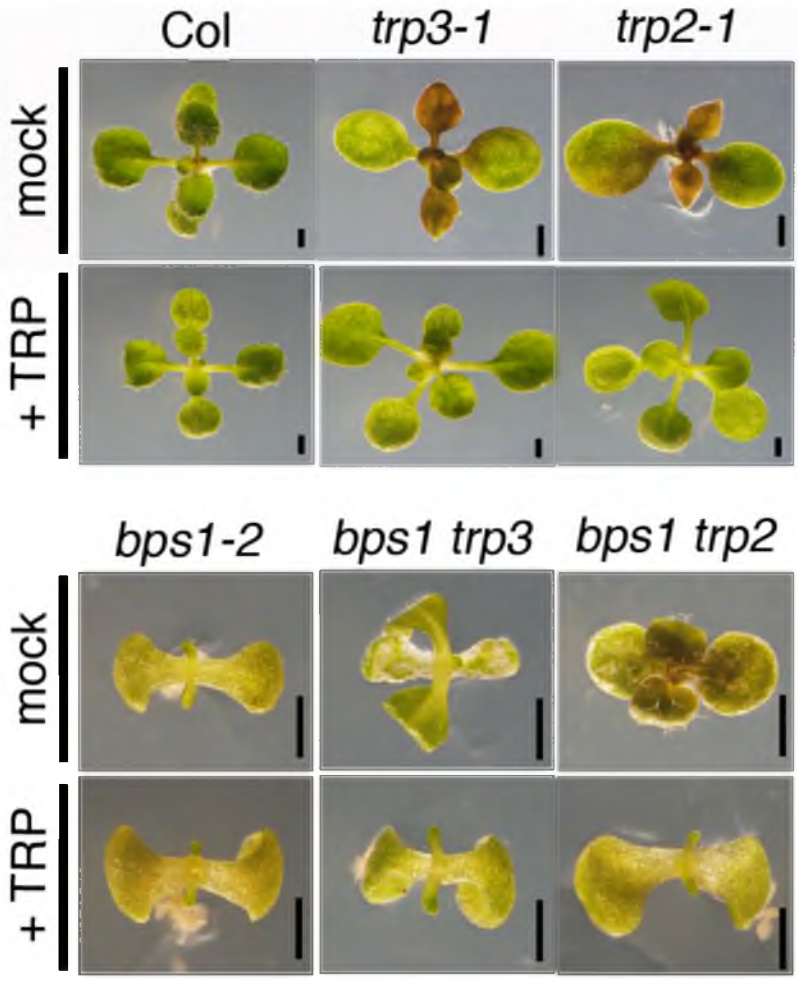

Figure 3.3: Phenotypes of *bps1 trp2 and bps1 trp3* mutants. Shown are images of 12 dpi seedlings grown on regular growth media (GM) or GM containing 250 µM Trp. WT (Col) had normal well-developed leaves with trichomes. *bps1-2* mutant produced small-radialized leaf primordia without trichomes. *trp3-1* and *trp2-1* mutants had smaller leaves than WT and they were pale in color. *trp3 bps1* and *trp2 bps1* double mutants developed well-developed leaves with trichomes and when they were grown on media supplemented with Trp, the seedlings were indistinguishable from *bps1*. Size bar = 1mm.

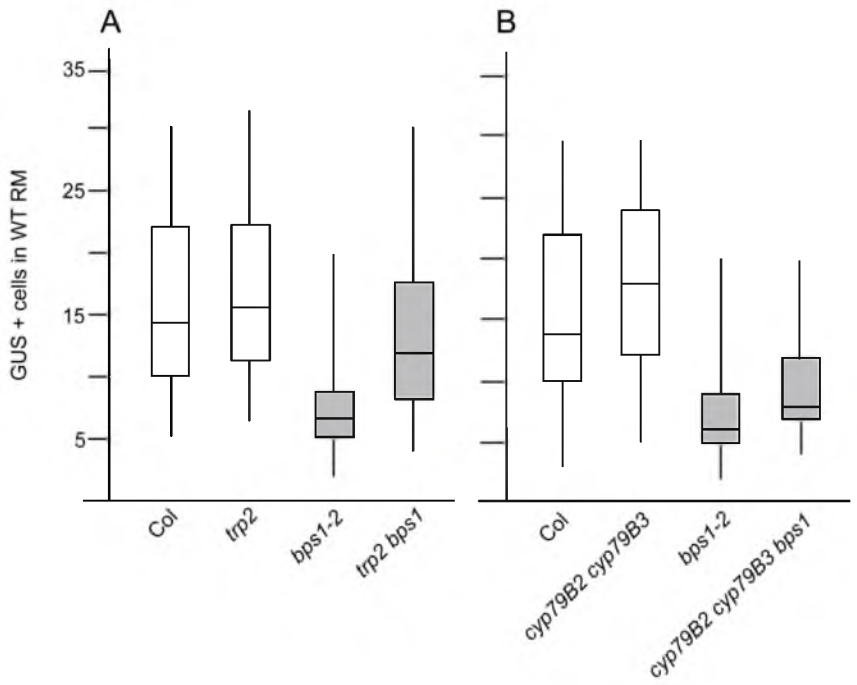

Figure 3.4: Bioassay quantification of *bps* signal shows that the *bps* signal is derived from Trp but not from IGs pathway. Box and whisker plots of the number of *pCYCB1;1::GUS*-stained cells in WT roots treated with extracts from several genotypes. (A) Quantitative measure of the *bps* signal activity. WT roots treated with extracts from controls, Col or *trp2,* had normal numbers of dividing cells. WT roots treated with extracts from *bps1-2* had reduced numbers of dividing cells, whereas those treated with extracts from *trp2 bps1* double mutants had increased numbers of dividing cells as compared to *bps1* extracts but slightly reduced than those treated with Col or *trp2* extracts. (B) Quantitative measure of the *bps* signal activity. WT roots treated with extracts from controls, Col or *cyp79B2 cyp79B3,* had normal numbers of dividing cells. WT roots treated with extracts from *bps1-2* had reduced numbers of dividing cells, whereas from *cyp79B2 cyp79B3 bps1* had similar numbers of dividing cells as *bps1-2*.

Table 3.1: Genetic analysis of *trp2 bps1* and *trp3 bps1* double mutants

Plants analyzed	Total (n)	WT-like and *trp*-like (n)	Predicted *bps1-2* like (n)	Observed *bps1-2* like (n)	Chi-square	Suppressed *bps1-2* (n)
Bps1-2/bps1-2	321	240	80.25	81	0.007	0
trp2-1/trp2-1;Bps1-2/bps1-2	306	229	76.5	20	41.72	57
trp3-1/trp3-1;Bps1-2/bps1-2	305	228	76.25	43	14.67	34

Hypothesis: There was no difference in the predicted and observed frequency of seedlings with *bps1*-like phenotype.
Chi-square value for seedlings with *bps1*-like phenotype was rejected. This indicated that the partial rescue of *bps1* mutants was statistically significant.

Chi-square values at 95% confidence is 3.841 when *df*= 1.
bps1-like phenotype = Seedlings with small, radialized leaves without trichomes.
Suppressed *bps1* = *bps1* seedlings that produced well-developed leaves with trichomes.

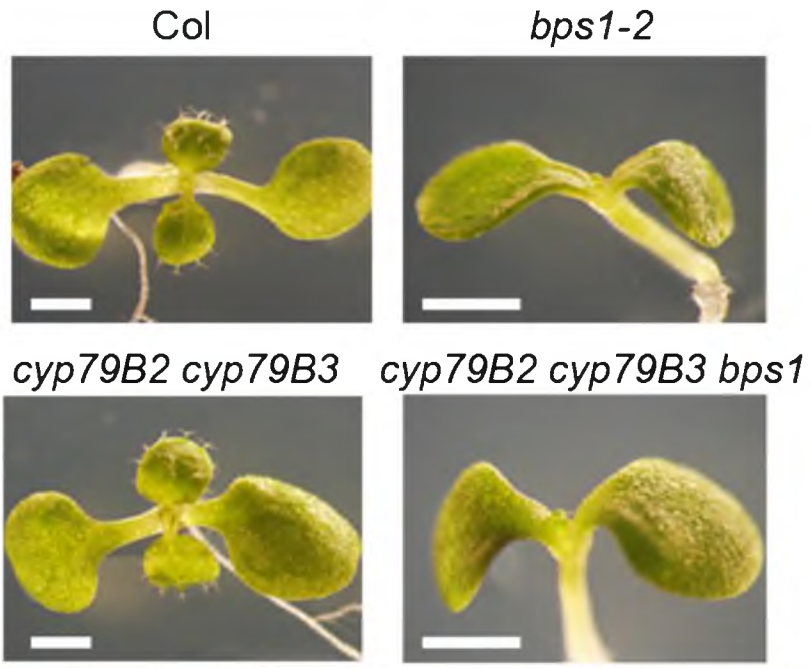

Figure 3.5: Seedling phenotypes of *cyp79B2 cyp79B3 bps1* triple mutants. Depicted here are 7 dpi seedlings. Col and *cyp79B2 cyp79B3* seedlings had normal well-developed leaves with trichomes. The *bps1-2* mutant produced small-radialized leaf without trichomes and the leaf development is arrested soon after initiation. The *cyp79B2 cyp79B3 bps1* triple mutant was indistinguishable from *bps1-2*. Size bar = 1mm.

CHAPTER 4

TOWARDS IDENTIFICATION OF THE *bps* SIGNAL

4.1 Abstract

The Arabidopsis *bypass1* (*bps1*) mutant roots overproduce a compound that is mobile and shows properties resembling a signaling molecule; we call this the *bps* signal. The *bps* signal is transported to the shoot and causes shoot arrest and also cause root defects. My primary goal was to carry out biochemical characterization and to work out purification strategies for the identification of the *bps* signal. Chemical characterization will be important, as it will allow us to determine when normal plants produce it. To characterize the *bps* signal chemically, we prepared aqueous extracts that were then subjected to a variety of fractionation procedures including SPE columns and HPLC, and mass spectrometry was used for compound detection. The partitioning of the *bps* signal was determined by using the bioassay. Using solid phase extraction (SPE) procedures, we show that the *bps* signal is a positively charged polar metabolite. Ultra Performance Liquid Chromatography (UPLC) was used for the fractionation and chemical separation was carried out using Hydrophilic Interaction Liquid Chromatography (HILIC). pHILIC (Ph9.2) and cHILIC (ph3.2) columns were used for the separation. Using a pHILIC analytical column, we identified one compound in the negative mode and two compounds in the positive mode MS detection as potential *bps* signal candidates. However, the active 30-second fraction, obtained from the pHILIC semipreparative column, did not contain these candidate compounds; instead it contained a different set of metabolites. When the 30-second active fraction was resolved using a different chemistry by employing a cHILIC analytical column, many additional compounds

were identified. This result suggested that ion suppression underestimated the composition of the 30-second active fraction, and that much more additional work is required before we can conclusively identify the *bps* signal.

4.2 Introduction

Metabolites are small organic compounds synthesized by organisms using enzyme-mediated chemical reactions[71]. Plants produce a variety of metabolites that are categorized into primary and secondary metabolites. Primary metabolites are compounds that are essential for growth and development and include carbohydrates, lipids, proteins, and nucleic acids. Secondary metabolites are generally nonessential for the basic metabolic processes but play a vital role in a plant's survival in the environment and include alkaloids, trepenoids, and phenolics[71,72]. Plants produce a staggering variety of secondary metabolites that play important roles in both defense and interaction with its environment. For example, floral scent volatiles and pigments have evolved to attract insect pollinators and thus enhance fertilization rates[73,74]. Chemicals found in fruits can act as signaling molecules by providing color, aroma, and flavor. These chemicals act as potential rewards for animals in the form of sugars, vitamins, and amino acids and help in seed dispersal[71]. Examples of metabolites that act in defense mechanisms against pests such as insects, pathogenic fungi, and bacteria are phenylpropanoids, isoprenoids, alkaloids, or fatty acid/polyketides[72]. There are other metabolites that are known to serve cellular functions, for examples resistance to drought, temperature, or salt[75]. In the condition of drought, endogenous ABA levels significantly increase, as revealed by

metabolite profiling. This then regulates the accumulation of various amino acids and sugars such as glucose and fructose[75,76]. In tolerance to temperature stress proline, monosaccharides (glucose and fructose), galactinol, and raffinose play important roles[77].

Because of the important functions performed by metabolites, an important goal in plant biology is to identify biologically active metabolites and to define their pathways. The pathways that produce many secondary metabolites have not yet been elucidated. The identification of metabolites in a particular pathway will be a step forward in clarifying the function of the pathway and the enzymes involved. However, identification of unknown metabolites is a technically challenging task. Several chromatographic methods including paper, thin layer, gas, ion exchange, and liquid have been used to identify plant metabolites. Recently, the new generation of analytical technologies, which include liquid chromatography (LC)- mass spectrometry (MS) and nuclear magnetic resonance (NMR), has been extensively used for the chemical identification[78].

4.2.1 Strategy for the *bps* signal identification

Our general strategy for the identification of the *bps* signal was to use chemical fractionation followed by a bioassay to identify which fraction contained the *bps* signal (Fig. 4.1). Metabolites were first extracted using MeOH: CHCL3: H2O as described in[44], and then fractionated using SPE. The SPE columns tested include reverse phase, normal phase, and ion exchange. Further purification was carried out using HPLC for eventual MS and MS/MS analysis.

First, we compared metabolite profiles of *bps1* single mutants with wild type. Significantly up-regulated metabolites in *bps1-1* and *bps1-2* in comparison to their respective wild types were sorted and assigned as a working metabolite list. We then examined metabolites of specialized genotypes. We analyzed metabolites from *bps1 trp2* and *bps1 cyp79B2 cyp79B3* mutants, because specific predictions could be made regarding the level of the *bps* signal. The *bps1 trp2* showed a suppressed phenotype, and the bioassay indicated reduced *bps* signal. In contrast, the *bps1 cyp79B2 cyp79B3* mutant has a normal severe phenotype and the bioassay indicated a normal level of the *bps* signal. These had altered secondary metabolite profiles that either contained or lacked a specific compound. Significantly altered metabolites were identified by comparing the compounds in the mutants and their respective wild types.

4.3 Material and methods

4.3.1 Plant material and growth conditions

The Arabidopsis thaliana Col, L *.er*, *bps1-2* (Col background), *bps1-1* (L *.er* background), *trp2-1*, *trp2-1 bps1-2*, *cyp79B2 cyp79B3*, and *cyp79B2 cyp79B3 bps1-2* were used for metabolite extraction. Seedlings were grown, as described in[40] and Chapter 3, at 22^{0}C in 24-hours light on petri-plates containing plant growth media (GM). In addition to regular media, *trp2-1* and *trp2-1 bps1-2* seedlings were also grown on GM supplied with 250 µM TRP (Sigma Aldrich). Aliquots of 50 mg of 7 dpi whole seedlings were placed in 2 ml tubes with 0.5 mm glass beads (MO BIO), flash-frozen in liquid nitrogen and were either used immediately for extraction or stored at -80^{0}C.

4.3.2 Crude metabolite extraction

We based our extraction protocol on one published by Giavaliso[79]. Our modifications include homogenization of tissue for 1 min using an Omni Bead Rupture 24 (Omni International). Hydrophilic metabolites were extracted from each aliquot using 1 ml of a mixture of cold methanol/water/chloroform (HPLC grade, Sigma-Aldrich) at 25:10:10 ratio (Fig. 4.1). Extraction was expedited by vigorous shaking for 20 min at 4^0C and then sonication (Branson 2510, Eppendorf) for 10 min at room temperature. After this, 250µl water was added, vortexed, and the tubes were spun down for 10 min at 1300 RCF in a tabletop centrifuge (Eppendorf). The supernatants, which contained polar compounds, were transferred to a fresh 1.5 ml microfuge tube. The sample was dried down in an *en vacuo* (Barnstead, Genevac).

4.3.3 Trapping the *bps* signal in an agarose block

Previously, we showed that the *bps* signal can exit the root, and cross an agarose block[44]. This observation provided us another method for isolating the *bps* signal, that is, by trapping it in an agarose block. To maximize the amount of trapped *bps* signal, silicon tubing containing 0.8 % agarose (Fisher Scientific, Molecular Biology Grade) in sterile water was set up with roots coming out both ends. Five 4 dpi L *.er* or *bps1-1* roots were inserted in the opposite ends of the silicon tubing (agarose approximately 0.5 mm in length). This set-up was maintained in sterile petri-plates containing GM with 1.5% agar for 24 hours. A no-root control was produced by maintaining an identical agarose block inside the silicon tubing and under the same conditions as the test samples. The

agarose blocks were taken out of the tubing and metabolites were extracted following the same method as used for seedlings. These extracts were also used for HPLC fractionation and MS analysis to identify the metabolites (Fig. 4.1).

4.3.4 Solid phase extraction (SPE)

SPE is a separation process by which compounds that are dissolved in a liquid solution are separated according to their physical and/or chemical properties. Compounds are separated based on their relative affinity for the solid phase of the column through which sample is passed, for example, based on charge or hydrophobicity. Our goal was to simplify the composition of the active metabolite extract. Therefore, SPE columns in which the fraction with the desired analyte (the *bps* signal) was retained in the stationary phase provided one round of purification. SPE columns are available in a wide variety of chemistries, such as reverse phase, normal phase, and ion exchange. All these three types of SPE columns were implemented for the separation of the *bps* signal from other compounds in the sample.

The reverses phase C-18 column (Discovery DSC-18, Sigma Aldrich) was employed for the fractionation of the crude extract. The column was washed and equilibrated with 4 ml MeOH and 4 ml H_2O, respectively, using a vacuum extraction manifold (Supelco). The vacuum was maintained at five HG. The crude extracts were suspended in 400 µl H_2O, loaded onto the column, and the column was washed with H_2O. The flow-through and the wash were pooled to make a single fraction, which we call flow-through. Finally, the remaining

metabolites were eluted with 100% MeOH. The flow-through and elute fractions were dried down *en vacuo*.

The normal phase ZIC-HILIC SPE column (SeQuant, The Nest Group) was also employed for fractionation of the crude extract. The column was washed with 2 ml H_2O and equilibrated with 2 ml MeOH, using a vacuum extraction manifold (Supelco). The vacuum was maintained at five HG. The crude extract was suspended in 400 µl 50% MeOH and was loaded onto the column. The column was washed with 50% MeOH; the flow-through and the wash were pooled together to make a single fraction. The metabolites that were retained in the column were eluted with H_2O. The flow-through and eluate fractions were dried down *en vacuo*.

To understand if the *bps* signal is a positively charged molecule, a mixed cation exchange (MCX) SPE column (Oasis, Waters) was employed. The column was washed and equilibrated with 1 ml MeOH and 1 ml 0.5% formic acid, respectively, using a vacuum extraction manifold (Supelco). The vacuum was maintained at five HG. The crude extracts were resuspended in 0.5% formic acid and were loaded onto the columns. The first wash of the column was carried out with 1 ml 0.1% formic acid. The flow-through and the first wash were pooled together to make a single fraction. This step was followed by a second wash by 1 ml MeOH. Finally, the metabolites were eluted with 1 ml 5% NH_4OH solution. The flow-through, MeOH wash, and eluate fractions were dried down *en vacuo*.

4.3.5 Sample preparation for LC-MS analysis

Dried samples, either C-18 flow-through or MCX eluate, which contained *bps* signal activity, were suspended in 50 µl of a 90% acetonitrile/10% 10mM ammonium formate solution for the pHILIC (pH9.2) and cHILIC (pH3.2) analytical columns. Samples were prepared using the same procedure for the pHILIC semi-preparative, except the suspension volume was 100 µl and the number of samples that were pooled together for each run was increased. A total of 12 crude extracts were run through the C-18 column and the flow-through was pooled together for each semipreparative run. For the purification using a MCX column, a total of 16 crude extracts were run through C-18; flow-through were collected and were run through the MCX columns. All the MCX eluate fractions were pooled together for each semipreparative run. The samples were vortexed, sonicated for 5 min, and centrifuged at 1400 RPM for 5 min. The supernatant was transferred to an auto-sampler vial and 2 µl or 20 µl of the sample was injected onto the analytical or semipreparative column, respectively.

4.3.6 LC-MS analytical analysis

An agilent 1290 liquid chromatography system consisting of two binary pumps, an auto sampler, and a column compartment was employed for sample analysis. Analytical columns, SeQuant ZIC-pHILIC and SeQuant ZIC-cHILIC, were used at basic pH (9.2) and acidic pH (3.2), respectively. The solvent system consisted of acetonitrile and 10 mM ammonium formate (pH9.2 or pH3.2). The liquid chromatography was programmed at 95% acetonitrile/5% 10 mM ammonium formate for 1 min followed by 20 min ramp to 40%

acetonitrile/60% 10 mM ammonium formate at 0.2 ml/min. An agilent 6550 QTOF was employed for mass spectrometric analysis. Each sample was run in both the positive and negative mode to fully capture the metabolome.

Targeted MS/MS-based experiments were performed to characterize potential metabolites that were altered in our screen. Fragmentation energy was 20 eV.

4.3.7 LC-MS semipreparative analysis

Semipreparative analysis was performed on an agilent 6520 UPLC-QTOF mass spectrometer system using a Merck SeQuant ZIC-pHILIC semipreparative column (150 x 4.6 mm). A two-solvent system was used for elution of the compounds and maintaining pH: acetonitrile (HPLC grade, Sigma-Aldrich) and 10 mM ammonium formate (pH 9.2) (HPLC grade, Fluka). 20 µl samples were injected from the auto-sampler. Initial column conditions were 95% acetonitrile/5% 10mM ammonium formate with a 1 min hold time; following this, a 20 min ramp to 40% acetonitrile/60% 10mM ammonium formate was performed. Flow rate was 1 ml/min. Following separation, the column was re-equilibrated for 20 min, a total run time of 46 min. Fractions of 0.8 ml were collected on a Biorad fraction collector using a flow-splitter with 0.8 ml/min to the fraction collector and 0.2 ml/min to the mass spectrometer.

4.3.8 Data analysis

Data were analyzed using a nontargeted approach. Files were filtered for noise and converted to .cef files using Mass Hunter Qualitative software. These

data were transferred to Mass Profiler Professional, which identifies metabolites whose abundance is altered with statistical significance. Recursive analysis was used to remove salt adducts and to produce a putative molecular formula. Further metabolite identification was performed using the METLIN database.

4.3.9 Statistical analysis

The Mann-Whitney U-test was used to test the statistical significant of the bioassay (i.e., numbers of *pCYCLB1;1::GUS*-stained cells following various treatments). This method was selected because the data are not normally distributed. In this method, a two-tailed probability measure was used for all the data analyzed; statistical significance was determined at *P*-value of <0.05.

4.4 Results

4.4.1 *bps* signal is a polar metabolite

The transient micrograft experiment showed that the *bps* signal exits the root, moves through the agarose plug, and then enters the shoot where it elicits a suite of responses[44]. Its ability to cross the aqueous agarose media strongly suggested it was a polar molecule. We verified the polar nature of the *bps* signal biochemically by determining how it fractionated on both normal and reverse phase SPE columns. C-18 is a reverse phase SPE column that contains C-18 hydrocarbons as the sorbent material. The organic solutes are partitioned from a mobile phase, such as water, into a nonpolar phase C-18 sorbent. The isolation is by a nonpolar interaction, called Van der Walls, dispersion forces, or partitioning. The analytes that are most hydrophobic have the greatest tendency

to bind to the C-18 sorbent and will be recovered in the eluate fraction[80]. If the *bps* signal was polar, we expected it to fail to adhere to the C-18 SPE column, and instead be recovered through the flow-through or waste fractions. Crude WT and *bps1* extracts were run through a C-18 column and the flow-through and eluate fractions were collected. The *bps* signal activities of the fractions were analyzed using the bioassay. The results showed that the *bps* signal activity of the *bps1* flow-through and control (unfractionated) *bps1* extracts were indistinguishable (Fig. 4.2A). In addition, we found no activity in the *bps1* eluate fraction, nor in either fraction of WT extracts (Fig. 4.2A). This result confirmed that the *bps* signal was polar.

We also confirmed the polar nature of the *bps* signal using a normal phase SPE column. ZIC-HILIC is a normal phase SPE column that contains a zwitterionic stationary phase (neutral molecule with a positive and a negative electric charge) covalently attached to porous silica. Molecules passing through this column are then separated based on polar interactions, such as hydrogen bonding, dipole-dipole interactions, and induced dipole-dipole interactions. Polar compounds bind to the sorbent material whereas nonpolar compounds present in the sample matrix do not bind to the sorbent and are obtained in the flow-through fraction[80]. If the *bps* signal was a polar molecule, we expected it to adhere to the ZIC-HILIC SPE column and to be recovered in the eluate fraction. WT and *bps1* crude extracts were collected. The *bps* signal activity of the fractions was analyzed using the bioassay. The bioassay result indicated that the *bps* signal activity of the *bps1* ZIC-HILIC eluate fraction was indistinguishable from the

control *bps1* extracts (Fig. 4.2B). The *bps* signal activity of the *bps1* ZIC-HILIC flow-through fraction was similar to that treated with WT extracts (Fig. 4.2B). This result further confirmed that the *bps* signal was a polar metabolite.

4.4.2 *bps* signal is a positively charged metabolite

A polar molecule is any molecule that has a net dipole as a result of the opposing charges (i.e., having partial positive and partial negative charges). Polarity is created whenever two atoms share electrons and one atom pulls electrons closer to itself. An excellent example of a polar molecule is water. Oxygen wants electrons more than hydrogen so it will pull electrons closer to it, causing the side of the molecule with the oxygen to be more negative[80]. To test if the *bps* signal is a positively or negatively charged compound, we fractionated crude extracts using a cation exchange SPE column. Cation exchange sorbents are derivatized with functional groups that interact with and retain positively charged molecules. MCX (mixed cation exchange) sorbent is a mixed-mode, reversed-phase/strong cation exchange polymer. Positively charged analytes bind to the sorbent material and the negative charged analytes are obtained in the flow-through[80]. If the *bps* signal was a positively charged molecule, we expected it to adhere to the MCX sorbent and be recovered following MCX elution using a base. *bps1* and WT crude extract was run onto the MCX column, the flow-through and the eluate fractions were collected, and the *bps* signal activity was tested. The *bps1* MCX flow-through fraction had *bps* signal activity similar to that treated with WT extracts (Fig. 4.2C). The *bps* signal activity was retained in the eluate, suggesting that the *bps* signal was a positively charged

metabolite.

4.4.3 Analysis of compounds detected in HPLC/MS runs

The use of SPE columns gave us several ways to enrich the *bps* signal, and these methods were used in conjunction with extracts from genotypes with predicted higher or lower levels of the *bps* signal (Chapter 3). The bioassay data suggested that the *bps* signal did not bind to the C-18 column but did bind to the HILIC and MCX columns. The next step was to partially purify the extracts using C-18 and MCX columns sequentially. The partially purified extracts were fractionated by HPLC using HILIC chromatography and MS identified metabolites. Metabolite profiles of *bps1-1*, *bps1-2*, Col, L *.er*, *cyp79B2 cyp79B3*, *cyp79B2 cyp79B3 bps1*, *trp2 bps1*, *trp2*, and *trp2* and *trp2 bps1* grown on Trp media (*trp2, trp2 bps1* + Trp) were analyzed in triplicates. Crude metabolite extracts from these genotypes were partially purified using SPE columns, either C-18 or C-18 and MCX, and were run through a pHILIC analytical column. Positive and negative mode MS was employed to identify the compounds.

Criteria for assigning the *bps* signal candidate were based on the phenotypes and bioassay results of the genotypes in study. We expected that the *bps1-1* and *bps1-2* would have a higher level of the compound as compared to their respective wild types L *.er* and Col. We anticipated that *bps cyp79B2 cyp79B3* triple mutants would have a higher level as compared to the *cyp79B2 cyp79B3* double mutants and a similar level as compared to *bps1-2*. *bps1-1* MCX eluate fractions and root exudates should contain a higher amount of the compound as compared to L *.er* MCX eluate and root exudates, respectively.

trp2 bps1-2 double mutants should have a lower amount of the compound as compared to *bps1-2* single mutant but should have a slightly higher amount than the controls, *trp2* and Col. The compounds that match all of our criteria were assigned as putative *bps* signal candidates.

Negative mode MS detected 19 metabolites in *bps1-2* and *bps1-1* samples that were altered in comparison to their respective wild types. Compounds that were altered by two-fold or higher were assigned as significant to avoid nonspecific alterations, which is common in metabolomics. Thirteen compounds were two-fold or higher in *bps1-2* and *bps1-1* as compared to Col and L *.er*, respectively (Table 4.1). If one of these was *bps* signal, then we expected that it would also be high in *cyp79B2 cyp79B3 bps1* mutants as compared to *cyp79B2 cyp79B3*. All the 13 compounds were two-fold or higher in *cyp79B2 cyp79B3 bps1* relative to *cyp79B2 cyp79B3* (Table 4.1). We next asked, out of these 13 compounds, how many were significantly higher in *bps1-1* MCX eluate as compared to L .er MCX eluate. Nine compounds were two-fold or higher in *bps1-1* MCX eluate as compared to L *.er* MCX eluate. Among nine compounds, three compounds were more than two-fold higher in *bps1-1* root exudates as compared to L *.er* root exudates (Table 4.1). Based on the above-mentioned analysis, three compounds were assigned as putative *bps* signal candidates.

Among three compounds, one compound was a candidate for the *bps* signal when we analyzed the data from *trp2 bps1* and *trp2 bps1* +Trp samples. The compound with m/z 316.0791 showed a trend to be higher in *bps1-2* as

compared to Col, lower in *trp2 bps1* than *bps1*, and again higher in *trp2 bps1* +Trp samples (Fig. 4.3). *trp2* mutants were used as a negative control and all the 12 compounds were detected at a lower level than *trp2 bps1*.

A total of 252 compounds were detected in the positive mode in *bps1-2* and *bps1-1* samples. Among them, 155 and 174 compounds were two-fold or higher in *bps1-1* and *bps1-2* as compared to L *.er* and Col, respectively (Table 4.2). One hundred and twenty-eight compounds were two-fold or higher in *cyp79B2 cyp79B3 bps1* as compared to *cyp79B2 cyp79B3*. Eighty-nine and 38 compounds were significantly higher in *bps1-1* MCX eluate and root exudates as compared to L *.er* MCX eluate and root exudates, respectively (Table 4.2). When we compared all the above criteria, 11 compounds showed a two-fold or higher level in both *bps1-1* and *bps1-2* as compared to WT throughout the samples analyzed, hence we assigned them as potential *bps* signal candidates (Table 4.2). Among these 11 compounds, two compounds showed a trend of being *bps* signal candidates when we analyzed the data from *trp2 bps1* and *trp2 bps1* +Trp samples. These compounds were higher in *bps1-2* as compared to Col, lower in *trp2 bps1* than *bps1*, and again higher in *trp2 bps1* +Trp samples (Fig. 4.4).

4.4.4 *bps* signal activity is retained in a 30-second fraction of the pHILIC semipreparative column

The analysis of metabolites using the pHILIC analytical column revealed one and two potential *bps* signal candidates in negative and positive modes, respectively. Because these compounds probably elute from the pHILIC at

different times, next we determined the time at which the *bps* single and these compounds elute. Finding that one compound eluted at the same time as a *bps* signal candidate would provide strong support for that compound being the *bps* signal. We fractionated the extracts using a pHILIC semipreparative column, then collected and tested the fractions for the *bps* signal activity using the bioassay. To test the feasibility of this approach, we first loaded the *bps* C-18 flow-through onto the pHILIC semipreparative column and tested each 5-min fraction for activity using the bioassay. The *bps* signal activity was only found in the 10-15-min fraction (Fig. 4.5A), indicating that this approach would help us to narrow down the candidates for the *bps* signal. The same result was obtained in all three replicates, giving us confidence on our approach.

To obtain fractions that contained fewer compounds, we ran the same type of preparative column, but during the 10-15-min time period, we collected fractions every 30 seconds. Testing of *bps* signal activity using the bioassay revealed that the 10.5-11-min fraction contained the *bps* signal (Fig. 4.5B). The experiment was replicated for three times and the results were consistent. To further narrow down the compounds present in a single fraction, we added another purification step. The *bps1* C-18 flow-through was run through the MCX column and the pHILIC semipreparative column was used to fractionate the MCX eluate. 30-second fractions were collected in between a 10-15-min time range. By bioassay, the 10.5-11-min fraction showed the *bps* signal activity (Fig. 4.5C), suggesting that one of the compounds in this fraction was the *bps* signal. The experiment was replicated for two times and the results were consistent.

4.4.5 Analysis of the compounds detected in 30-second active fraction by an alternative HILIC column

The active 30-second fraction of the *bps1* most pure sample (run through C-18 and MCX SPE columns), obtained from the pHILIC semipreparative column, had in total three compounds in the positive mode and none in the negative mode based on two replicas. All three compounds were higher in *bps1-1* as compared to L *.er*. However, these three compounds were different than the 11 *bps* signal candidates obtained from the analytical column analysis (Table 4.3). The possibility was that fewer compounds might have been detected in the 30-second fraction due to ion suppression. To further detect more compounds in the 30-second active fraction, which may not have been detected due to ion suppression, we employed another step of separation. The 30-second fraction collected from the pHILIC semipreparative column was run through a cHILIC (pH 3.2) analytical column in two replicates.

Negative mode MS detected 23 and 16 compounds in *bps1-1* and L *.er*, respectively. Eleven compounds were identified in both genotypes and among them, three compounds were 2 fold or higher in *bps1-1*. Out of 23 compounds that were detected in *bps1-1*, 12 compounds were detected only in *bps1-1.* A total of 15 compounds proved to be the potential *bps* signal candidates (Table 4.5).

Positive mode MS detected 308 and 141 compounds in *bps1-1* and L *.er*, respectively. Thirty-six compounds were common in both the genotypes and among them, nine compounds proved to be the potential *bps* signal; they were 2

fold or higher in *bps1-1*. Out of 308, 272 compounds were detected only in *bps1-1*. A total of 281 compounds proved to be the potential *bps* signal candidates. Among 15 compounds in the negative mode and 281 in the positive mode, to find out which single compound is the *bps* signal, further analysis is required.

4.6 Discussion

Arabidopsis *bps1* mutant roots overproduce a small metabolite, *bps* signal, which arrests shoot development and causes abnormal root development. The main goal of the project described here is to carry out biochemical characterization and to work out purification strategies for the identification of the *bps* signal. The strategy we employed was to partially purify the crude extracts by SPE columns, fractionate the extracts using HPLC, find out the active fraction by using the bioassay, and finally detect the compounds by MS.

Previous work using transient micrograft experiments revealed that the *bps* signal exits the *bps1* root, enters the agarose plug and then enters the shoot. This result suggested that the *bps* signal was a polar molecule. To biochemically characterize the polar nature of the *bps* signal, we used the SPE fractionation method. We used two different types of SPE columns: reverse phase C-18 and normal phase ZIC-HILIC. The *bps* signal did not bind to the C-18 column but it did bind to ZIC-HILIC column, as revealed by the bioassay, confirming that it is a polar molecule. A polar molecule has a net dipole as a result of opposing charges. So, it is possible that the *bps* signal could be either a positively or negatively charged compound; we fractionated the *bps1* extracts using mixed cation exchange (MCX) column. Cation exchange sorbent contains functional

groups that interact and retain positively charged molecules. The *bps* signal was retained in the MCX column, as measured by the bioassay, suggesting that it is a positively charged compound. The finding that the *bps* signal binds to a ZIC-HILIC SPE column provided us a method to further fractionate the extracts by HPLC using HILIC chromatography. The C-18 and MCX SPE column gave us ways to partially purify the crude extracts and enrich the *bps* signal.

To identify the potential *bps* signal candidates, we purified the extracts from several genotypes that had altered numbers and levels of metabolites by HPLC using pHILIC analytical column. We analyzed the overall metabolite profiles of *bps1-1*, *bps1-2*, *trp2 bps1*, and *cyp79B2 cyp79B3 bps1* mutants and their respective wild types. We show that 19 and 252 metabolites, respectively in negative and positive mode, were altered in *bps1* mutants as compared to the wild type. Further analysis of the metabolite profiles of *trp2 bps1* and *cyp79B2 cyp79B3 bps1* revealed one compound in negative mode and two compounds in positive mode to be putative *bps* signal candidates. If one particular compound among these compounds was *bps* signal, we reasoned that the fraction containing that compound would give us *bps* signal activity.

We employed the pHILIC semipreparative column and collected a 5-min fraction. A single 10-15-min fraction gave the *bps* signal activity. This active 5-min fraction contained a lot of compounds when detected by negative mode or positive mode MS. It was not feasible to assign one particular compound among so many compounds as a potential *bps* signal candidate. So, to further narrow down and limit the numbers of compounds present in a single fraction, we

collected 30-second fractions during a 10-15-min time period. We show that a single 30-second fraction, 10.5-11 min, contained the *bps* signal activity, suggesting that fraction contains the *bps* signal. We show that the 30-second active fraction contained a total of three compounds in positive mode MS and none in negative mode MS. But these three compounds, detected by positive mode MS, were different compounds than the two potential *bps* signal candidates that were revealed by the pHILIC analytical column analysis. The possibility was that fewer compounds might have been detected in the 30-second active fraction due to ion suppression. To further detect more compounds in the 30-second active fraction, we employed another step of separation. Using a cHILIC analytical column, we show that the 30-second active fraction contained 23 compounds when detected by negative mode MS and 308 compounds when detected by positive mode; 281 compounds proved to be potential bps signal candidates. Further analysis is required to find one particular compound that will give *bps* signal activity. The cHILIC preparative column could be used to fractionate the 30-second active fraction. The fractions collected from the cHILIC preparative column could be tested for the *bps* signal activity, and we can narrow down the list of potential *bps* signal candidates.

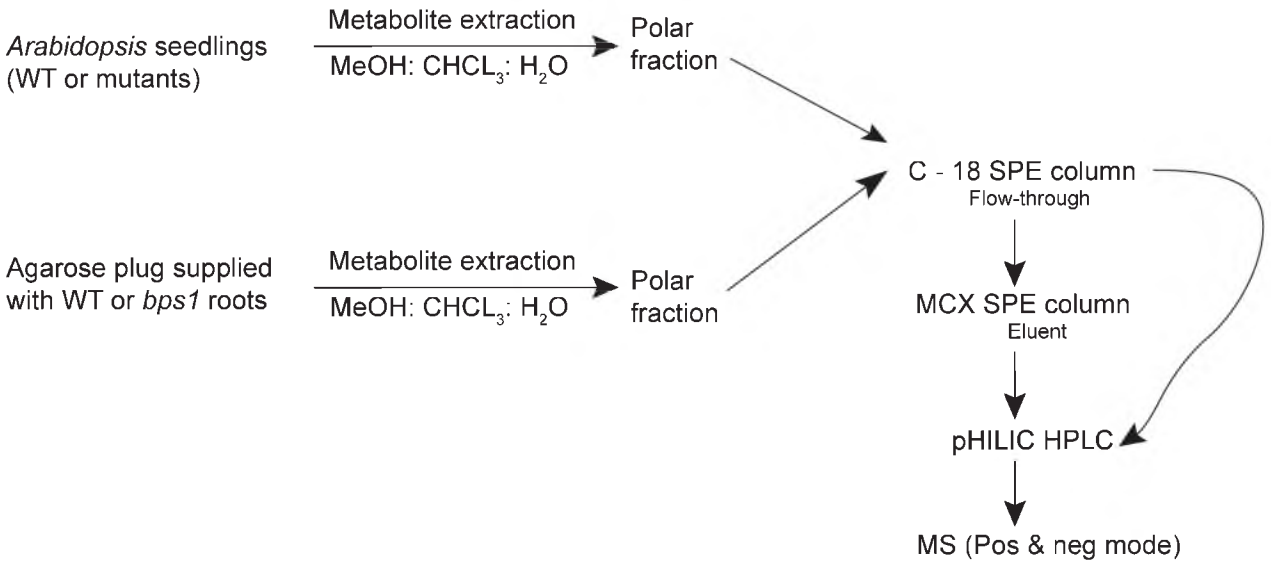

Figure 4.1: Flow chart of experimental procedures. Metabolites were extracted from several genotypes, partially purified using several SPE columns, and finally run onto HPLC-MS.

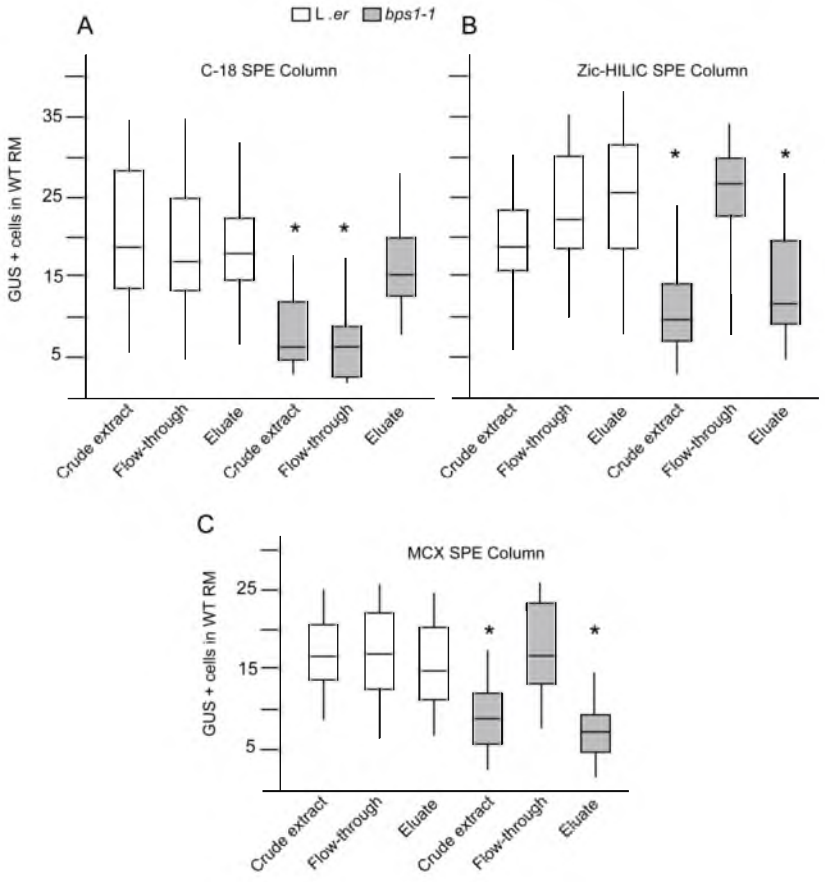

Figure 4.2: Biochemical characterization of *bps* signal using SPE columns. Box-plot show numbers of *pCYCB1;1::GUS*-stained cells in the wild type (WT) root meristem (RM). Boxes delineate the data points falling between 25% and 75%, the line bisecting the box shows the median, and the whiskers indicate the highest and lowest data point. WT seedlings were treated with WT (L *.er*) and *bps1-1* extracts run through the C-18 column (A), Zic-HILIC SPE column (B), and MCX SPE column (C). * Indicate statistically significant (Mann-Whitney U-test, $p < 0.05$).

Table 4.1: Fold change of compounds that were detected by MS using negative mode.
Listed are the compounds that were altered between *bps1* and WT based on biological triplicates. Highlighted in green are compounds that meet the criteria of being the *bps* signal.

		bps1-2 / Col (C-18 flow-through)	*bps1-1* / L *.er* (C-18 flow-through)	*cyp79B2 cyp79B3 bps1/ cyp79B2 cyp79B3* (C-18 flow-through)	*bps1-1* / L *.er* (MCX eluate)	*bps1-1* / L *.er* (Root exudates)
RT	**m/z**	**FC**	**FC**	**FC**	**FC**	**FC**
9.170	259.0698	10.970	3.611	6.740	17.985	ND
10.660	466.1361	17.638	19.508	16.423	11.967	ND
10.690	286.0713	4.443	5.067	13.541	82.199	70.792
10.690	594.1225	474832.177	292127.489	202432.195	936.136	ND
10.690	368.1134	0.076	0.107	0.088	0.047	0.271
10.770	164.0689	0.281	0.383	0.468	1.397	0.034
11.120	211.0521	3.140	2.115	3.670	ND	8.255
11.250	138.0322	628.191	362.052	415.375	64.450	2.046
11.250	94.0423	985.239	140.973	129.144	130.397	1.043
11.260	600.1742	21645.674	471711.110	146377.664	18.727	ND
11.269	186.0302	11.045	6.421	5.031	ND	ND
11.460	956.1463	213.777	6527.986	40.333	ND	ND
11.560	210.0739	2.038	1.711	2.660	0.561	ND
11.600	316.0791	347.621	119.163	91.342	17326.557	207.318
11.710	166.0487	2.844	2.576	2.812	1.401	0.447
11.860	163.0304	89.585	137.364	11.895	15247.597	ND
12.220	168.029	0.104	0.211	0.248	0.030	ND
12.310	680.1719	0.075	0.046	0.122	0.009	ND
12.550	340.0919	0.644	0.281	0.555	1.788	ND

RT = Retention time
FC = Fold Change
ND = Not detected

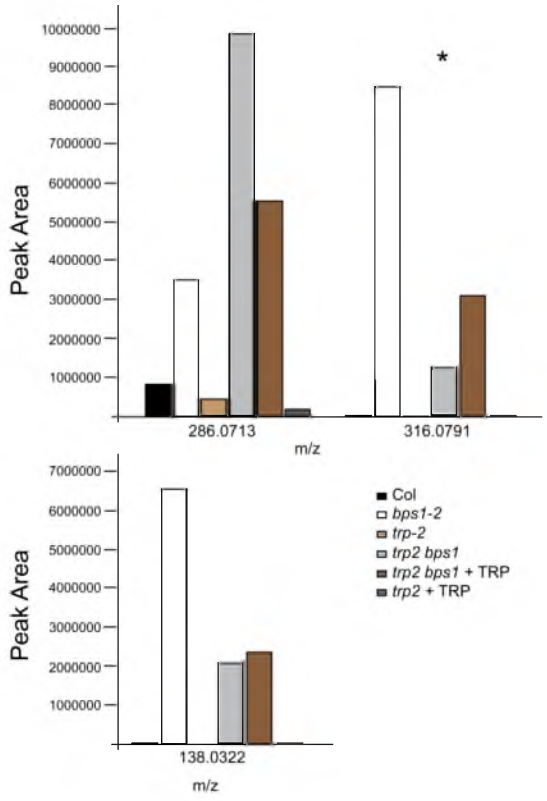

Figure 4.3: Quantification of three *bps* signal candidates obtained from negative mode analysis in *trp2 bps1* mutants. Depicted here is the peak analysis of metabolites from *trp2 bps1* seedlings grown on Trp media. Col, *bps1-2*, *trp2*, *trp2 bps1*, and *trp2*+Trp serve as controls. If one of the compounds was the *bps* signal, we predicted that the compound was significantly high in *bps1-2,* low in *bps1 trp2* as compared to *bps1*, and when *bps1 trp2* seedlings were supplied with exogenous Trp, the level of the compound was increased.

* Indicates that the compound matched our criteria of being the *bps* signal.

Table 4.2: Analysis of the number of compounds that were considered significantly up-regulated. Compounds in C-18 flow-through, MCX eluate, or root exudates were separated using pHILIC analytical column and were detected by positive mode MS. The total compounds detected, and the number of compounds that were two-fold or higher in mutants as compared to their respective wild types based on biological triplicates, is indicated.

Genotypes	No. of compounds (2 fold or higher)	Total compounds
bps1-1 / L *.er* (C-18 flowthrough)	155	252
bps1-2 / Col (C-18 flowthrough)	174	252
cyp79B2 cyp79B3 bps1 / *cyp79B2 cyp79B3* (C-18 flowthrough)	128	252
bps1-1 / L *.er* (MCX eluate)	89	252
bps1-1 / L *.er* (Root exudates)	38	252
Compounds significant throughout all the samples	11	252

Table 4.3: Fold change analysis of potential *bps* signal candidates that were obtained from positive mode MS. Listed are the compounds that meet all the criteria of being the *bps* signal based on biological triplicates.

		bps1-2 / Col (C-18 flow-through)	*bps1-1* / L .*er* (C-18 flow-through)	*cyp79B2 cyp79B3 bps1/ cyp79B2 cyp79B3* (C-18 flow-through)	*bps1-1* / L .*er* (C-18 +MCX)	*bps1-1* / L .*er* (Root exudates) Crude
RT	**m/z**	**FC**	**FC**	**FC**	**FC**	**FC**
6.669	388.1612	7.784	28.758	22.954	3.132	4.647
9.065	77.0393	4.878	2.737	3.138	3.189	2.833
9.114	120.0832	4.862	3.429	4.089	4.604	3.512
9.215	177.0563	7.440	2.553	10.018	3.719	24.665
10.387	284.1003	2.488	4.450	3.807	4.528	25.159
10.768	411.1291	4.539	6.381	5.256	2.632	3.445
11.151	256.0854	31.860	13.447	7.448	62.943	3.681
11.180	308.1352	142.586	107.803	39.103	5.135	28.423
11.254	339.051	374.097	127.671	137.539	32.112	27.443
11.268	323.0747	246.582	134.144	74.192	26.656	2395.727
13.547	313.0797	11.054	12.059	4.366	229.247	55.608

RT = Retention time
FC = Fold Change

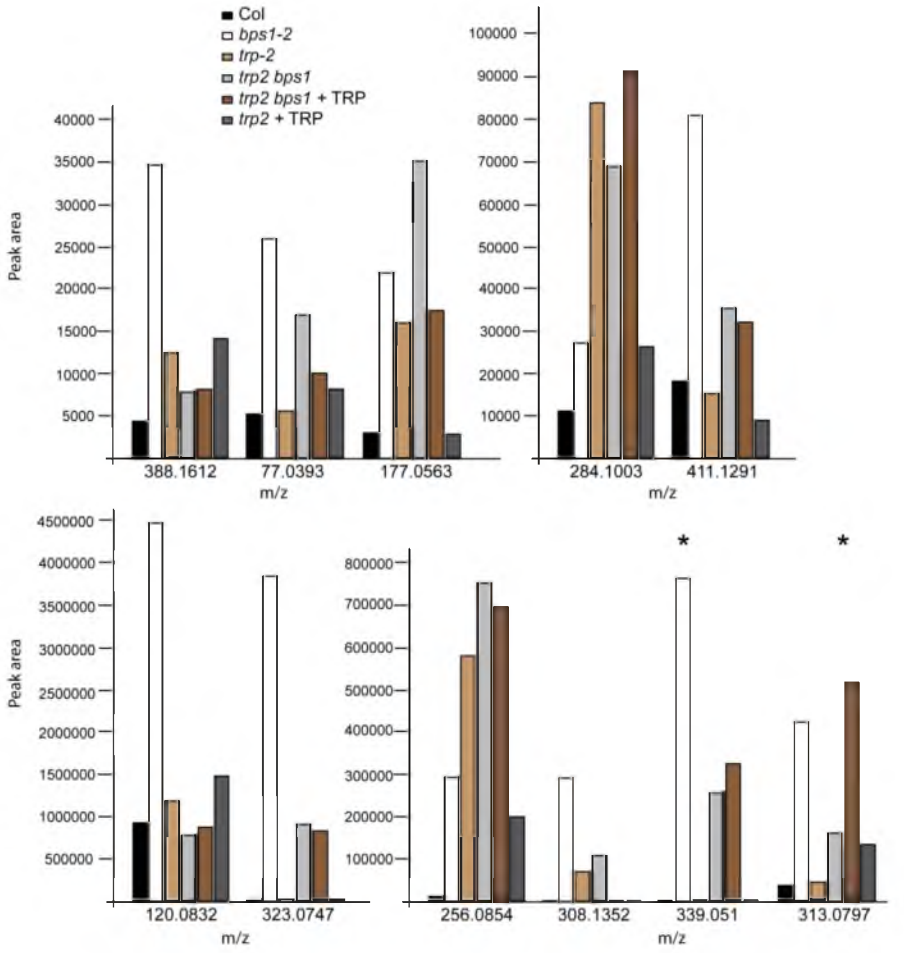

Figure 4.4: Quantification of 11 *bps* signal candidates obtained from positive mode MS in *bps1 trp2* mutants. Depicted here is the peak analysis of metabolites from *trp2 bps1* seedlings grown on Trp media. Col, *bps1-2*, *trp2*, *trp2 bps1*, and *trp2*+Trp serve as controls. If one of the compounds was the *bps* signal, we predicted that the compound was significantly high in *bps1-2,* low in *bps1 trp2* as compared to *bps1*, and when *bps1 trp2* seedlings were supplied with exogenous Trp, the level of the compound was increased. * Indicates that the compounds meet the criteria for being the *bps* signal.

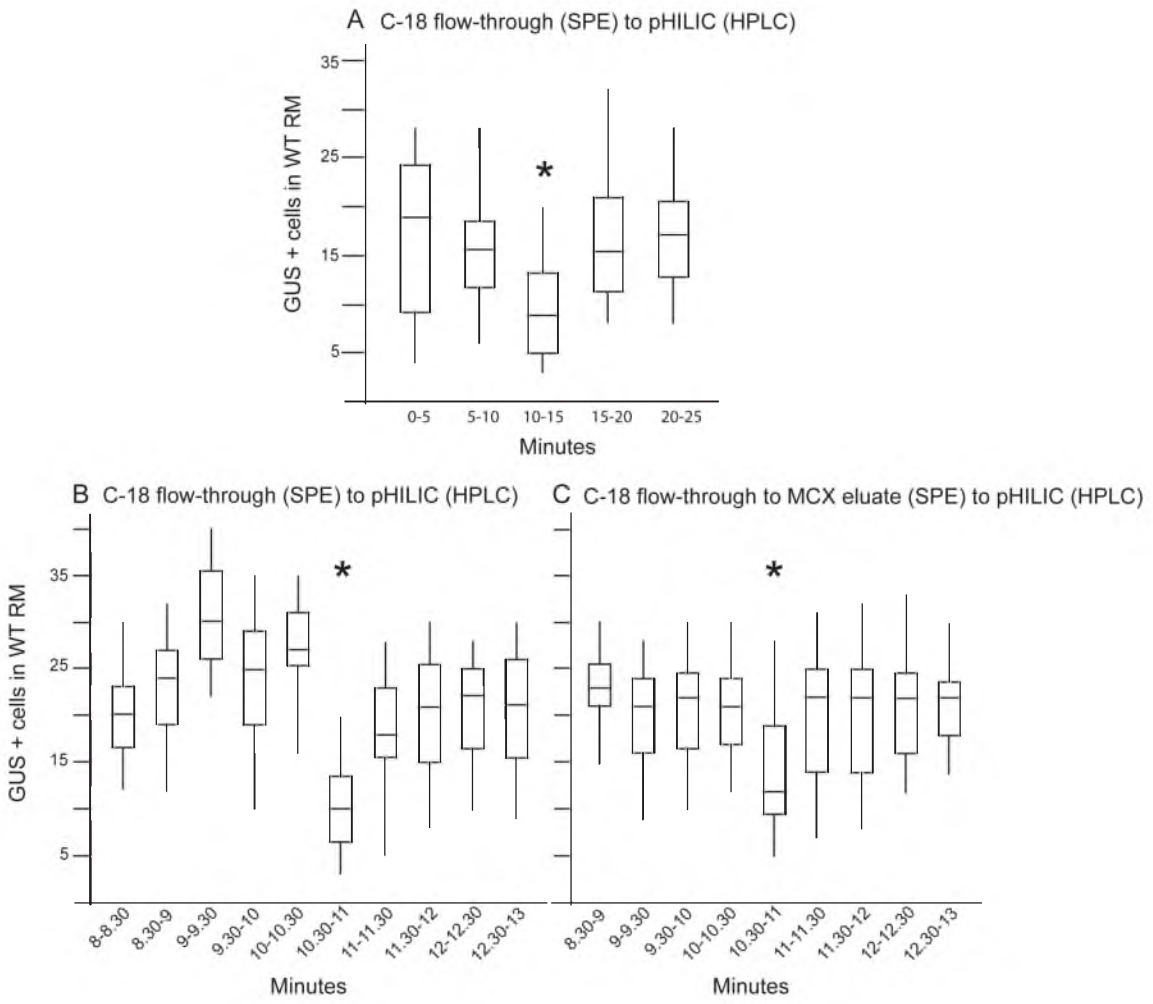

Figure 4.5: Test of the *bps* signal activity of fractions from the pHILIC semipreparative column. Crude extract was run through a C-18 SPE column, the flow-through was run onto a pHILIC semipreparative column, and the activity of 5-min fractions (A) and 30-second fractions (B) were tested. (C) Crude extract was run through a C-18 SPE column and the flow-through was run through a MCX SPE column. The eluate fraction was run onto the pHILIC semipreparative column and the *bps* signal activity of each 30-second fraction was tested. * Indicates statically significant (Mann- Whitney U-test, $p < 0.05$).

Table 4.4: Compounds detected by positive mode MS in the *bps1* 30-second active fraction. A total of three compounds were detected in the active 30-second *bps1* fraction obtained from the pHILIC semipreparative column. All three compounds were significantly higher in *bps1-1* than in L *.er*.

Renention time	m/z	Volume L *.er*	Volume *bps1-1*
10.434	229.1547	ND	245022
10.667	233.1241	252573	466534
11.045	144.0658	ND	769011

ND = Not detected

Table 4.5: Analysis of the number of compounds present in the active 30-second fraction. The active 30-second fraction obtained from pHILIC semi-preparative column was run through a cHILIC analytical column and the compounds were detected by both positive and negative mode MS.

	Negative mode		Positive mode	
	bps1-1	L *.er*	*bps1-1*	L *.er*
Total compounds detected	23	16	308	141
Compounds detected only in *bps1*	12		272	
Compounds detected only in L *.er*		5		105
Compounds detected in both	11	11	36	36
Compounds that are 2 fold or higher in *bps1*	3		9	
Total number of potential *bps* signal candidates	**15**		**281**	

REFERENCES

1. Mulligan, R., Chory, J. & Ecker, J. Signaling in plants. *Proc. Natl Acad. Sci. USA* **94,** 2793–2795 (1997).

2. Santner, A. & Estelle, M. Recent advances and emerging trends in plant hormone signalling. *Nature* **459,** 1071–8 (2009).

3. Leyser, O. The power of auxin in plants. *Plant Physiol.* **154,** 501–5 (2010).

4. Benjamins, R. & Scheres, B. Auxin: The looping star in plant development. *Annu. Rev. Plant Biol.* **59,** 443–65 (2008).

5. Wasilewska, A. *et al.* An update on abscisic acid signaling in plants and more... *Mol. Plant* **1,** 198–217 (2008).

6. Mok, D. & Mok, M. Cytokinin metabolism and action. *Annu. Rev. Plant Physiol.* **52**, 89–118 (2001).

7. Kudo, T., Kiba, T. & Sakakibara, H. Metabolism and long-distance translocation of cytokinins. *J. Integr. Plant Biol.* **52,** 53–60 (2010).

8. Takei, K., Sakakibara, H., Taniguchi, M. & Sugiyama, T. Nitrogen-Dependent Accumulation of Cytokinins in Root and the Translocation to Leaf : Implication of Cytokinin Species that Induces Gene Expression of Maize Response Regulator. *Plant Cell Physiol.* **42,** 85–93 (2001).

9. Yamaguchi, S. Gibberellin metabolism and its regulation. *Annu. Rev. Plant Biol.* **59,** 225–51 (2008).

10. Davière, J-M. & Achard, P. Gibberellin signaling in plants. *Development* **140,** 1147–51 (2013).

11. Leyser, O. Strigolactones and shoot branching: a new trick for a young dog. *Dev. Cell* **15,** 337–8 (2008).

12. Gomez-Roldan, V. *et al.* Strigolactone inhibition of shoot branching. *Nature* **455,** 189–94 (2008).

13. Umehara, M. *et al.* Inhibition of shoot branching by new terpenoid plant hormones. *Nature* **455,** 195–200 (2008).

14. Grant, M. & Lamb, C. Systemic immunity. *Curr. Opin. Plant Biol.* **9,** 414–20 (2006).

15. Katsir, L., Davies, K. A, Bergmann, D. C. & Laux, T. Peptide signaling in plant development. *Curr. Biol.* **21,** R356–64 (2011).

16. Choudhury, S., Panda, P., Sahoo, L. & Panda, S. K. Reactive oxygen species signaling in plants under abiotic stress. *Plant Signaling & Behavior* **8**, e23681-6 (2013).

17. Miller, G. *et al.* The plant NADPH oxidase RBOHD mediates rapid systemic signaling in response to diverse stimuli. *Sci. Signl.* **2,** 1-10 (2009).

18. Sevilem, I., Miyashima, S. & Helariutta, Y. Cell-to-cell communication via plasmodesmata in vascular plants. *Cell Adh. Migr.* **7,** 27–32 (2013).

19. Brand, U. Dependence of Stem Cell Fate in Arabidopsis on a Feedback Loop Regulated by CLV3 Activity. *Science* **289,** 617–619 (2000).

20. Schoof, H. *et al.* The stem cell population of Arabidopsis shoot meristems in maintained by a regulatory loop between the CLAVATA and WUSCHEL genes. *Cell* **100,** 635–44 (2000).

21. Stahl, Y. & Simon, R. Is the Arabidopsis root niche protected by sequestration of the CLE40 signal by its putative receptor ACR4? *Plant Signal. Behav.* **4,** 634–5 (2009).

22. Hirakawa, Y. *et al.* Non-cell-autonomous control of vascular stem cell fate by a CLE peptide/receptor system. *Proc. Natl. Acad. Sci. USA* **105,** 15208–13 (2008).

23. Carlsbecker, A. *et al.* Cell signalling by microRNA165/6 directs gene dose-dependent root cell fate. *Nature* **465,** 316–21 (2010).

24. Chitwood, D. H. *et al.* Pattern formation via small RNA mobility. *Genes & Development* **23,** 549–554 (2009).

25. Lin, W-Y., Huang, T-K., Leong, S. J. & Chiou, T-J. Long-distance call from phosphate: systemic regulation of phosphate starvation responses. *J. Exp. Bot.* **65,** 1817–27 (2014).

26. Turnbull, C. G. N. & Lopez-cobollo, R. M. Heavy traffic in the fast lane : long-distance signalling by macromolecules. *New Phytologist* **198,** 33–51 (2013).

27. Schachtman, D. P. & Goodger, J. Q. D. Chemical root to shoot signaling under drought. *Trends Plant Sci.* **13,** 281–7 (2008).

28. Zhang, Z., Liao, H. & Lucas, W. J. Molecular mechanisms underlying phosphate sensing, signaling, and adaptation in plants. *J. Integr. Plant Biol.* **56,** 192–220 (2014).

29. Chiou, T-J. & Lin, S-I. Signaling network in sensing phosphate availability in plants. *Annu. Rev. Plant Biol.* **62,** 185–206 (2011).

30. Banerjee, A. K. *et al.* Dynamics of a mobile RNA of potato involved in a long-distance signaling pathway. *Plant Cell* **18,** 3443–57 (2006).

31. Hannapel, D. J., Sharma, P. & Lin, T. Phloem-mobile messenger RNAs and root development. *Front. Plant Sci.* **4,** 257 (2013).

32. Bari, R., Pant, B. D., Stitt, M. & Golm, S. P. Phosphate-Signaling Pathway in Plants. *Plant Physiol.* **141,** 988–999 (2006).

33. Marín-González, E. & Suárez-López, P. "And yet it moves": cell-to-cell and long-distance signaling by plant microRNAs. *Plant Sci.* **196,** 18–30 (2012).

34. Li, D., Kinkema, M. & Gresshoff, P. M. Autoregulation of nodulation (AON) in Pisum sativum (pea) involves signalling events associated with both nodule primordia development and nitrogen fixation. *J. Plant Physiol.* **166,** 955–67 (2009).

35. Ferguson, B. J. *et al.* Molecular analysis of legume nodule development and autoregulation. *J. Integr. Plant Biol.* **52,** 61–76 (2010).

36. Svistoonoff, S. *et al.* Root tip contact with low-phosphate media reprograms plant root architecture. *Nat. Genet.* **39,** 792–6 (2007).

37. Saab, I. & Sharp, R. Non-hrdyaulic signals fron maize roots in drying soil: inhibition of leaf elongation but not stomatal conductance. *Planta* **179,** 466-474 (1989)

38. Smet, I., Voss, U., Jürgens, G. & Beeckman, T. Receptor-like kinases shape the plant. *Nat. Cell Biol.* **11,** 1166–73 (2009).

39. Shiu, S-H. & Bleecker, A. Receptor-like kinases from Arabidopsis form a monophyletic gene family related to animal receptor kinases. *Proc. Natl. Acad. Sci. USA* **98,** 10763–8 (2001).

40. Van Norman, J. M., Frederick, R. L. & Sieburth, L. E. BYPASS1 negatively regulates a root-derived signal that controls plant architecture. *Curr. Biol.* **14,** 1739–46 (2004).

41. Vernoux, T. *et al.* The ROOT MERISTEMLESS1/CADMIUM SENSITIVE2 gene defines a glutathione-dependent pathway involved in initiation and maintenance of cell division during postembryonic root development. *Plant Cell* **12,** 97–110 (2000).

42. Cheng, J. C., Seeley, K. A. & Sung, Z. R. RML1 and RML2, Arabidopsis genes required for cell proliferation at the root tip. *Plant Physiol.* **107,** 365–76 (1995).

43. Van Norman, J. M., Murphy, C. & Sieburth, L. E. BYPASS1: synthesis of the mobile root-derived signal requires active root growth and arrests early leaf development. *BMC Plant Biol.* **11,** 28 (2011).

44. Adhikari, E., Lee, D.-K., Giavalisco, P. & Sieburth, L. E. Long-distance signaling in bypass1 mutants: bioassay development reveals the bps signal to be a metabolite. *Mol. Plant* **6,** 164–73 (2013).

45. Van Norman, J. M. & Sieburth, L. E. Dissecting the biosynthetic pathway for the bypass1 root-derived signal. *Plant J.* **49,** 619–28 (2007).

46. Bernard, H. *et al.* Construction of plasmid cloning vehicles that promote gene expression from the bacteriophase lamda PL promoter. *Gene* **1,** 59-76 (1979).

47. Radwanski, E. & Robert, L. Tryptophan Biosynthesis and Metabolism: Biochemical and Molecular Genetics. *The Plant Cell* **7,** 921–934 (1995).

48. Kutchan, T. M. Alkaloid Biosynthesis -The Basis for Metabolic Engineering of Medicinal Plants. *The Plant Cell* **7,** 1059–1070 (1995).

49. Niyogi, K. K. & Fink, G. R. Two anthranilate synthase genes in Arabidopsis: defense-related regulation of the tryptophan pathway. *The Plant Cell* **4,** 721–33 (1992).

50. Niyogi, K. K., Last, R. L., Fink, G. R. & Keith, B. Suppressors of trp1 fluorescence identify a new arabidopsis gene, TRP4, encoding the anthranilate synthase beta subunit. *The Plant Cell* **5,** 1011–27 (1993).

51. Rose, A., Casselman, A. & Last, R. A Phosphoribosylanthranilate Transferase Gene Is Defective in Blue Fluorescent Arabidopsis thaliana Tryptophan Mutants. *Plant Physiol.* **100,** 582–92 (1992).

52. Li, J., Zhao, J., Rose, A. B., Schmidt, R. & Last, R. L. Arabidopsis Phosphoribosylanthranilate Isomerase : Molecular Genetic Analysis of Triplicate Tryptophan Pathway Genes. *The Plant Cell* **7,** 447–461 (1995).

53. Li, J., Chen, S., Zhu, L. & Last, R. Isolation of cDNAs encoding the tryptophan pathway enzyme indole-3-glycerol phosphate synthase from Arabidopsis thaliana. *Plant Physiol.* **108,** 877–8 (1995).

54. Berlyn, M. B., Last, R. & Fink, G. R. A gene encoding the tryptophan synthase I3 subunit of Arabidopsis thaliana. *Proc. Natl. Acad. Sci. USA* **86,** 4604–4608 (1989).

55. Last, R., Bissinger, P. H., Mahoney, D. J., Radwanski, E. & Fink, G. Tryptophan mutants in Arabidopsis: the consequences of duplicated tryptophan synthase beta genes. *The Plant Cell* **3,** 345–58 (1991).

56. Berlyn, M., Last, R. & Fink, R. A gene encoding the tryptophan synthase beta subunit of Arabidopsis thaliana. *Proc. Natl. Acad. Sci. USA* **86,** 4604–8 (1989).

57. Last, R., Bissinger, P. H., Mahoney, D. J., Radwanski, E. & Fink, G. Tryptophan Mutants in Arabidopsis: The Consequences of Duplicated Tryptophan Synthase b Genes. *The Plant Cell* **3,** 345 (1991).

58. Hull, a K., Vij, R. & Celenza, J. L. Arabidopsis cytochrome P450s that catalyze the first step of tryptophan-dependent indole-3-acetic acid biosynthesis. *Proc. Natl. Acad. Sci. USA* **97,** 2379–84 (2000).

59. Mikkelsen, M. D., Hansen, C. H., Wittstock, U. & Halkier, B. a. Cytochrome P450 CYP79B2 from Arabidopsis catalyzes the conversion of tryptophan to indole-3-acetaldoxime, a precursor of indole glucosinolates and indole-3-acetic acid. *J. Biol. Chem.* **275,** 33712–7 (2000).

60. Zhao, Y. *et al.* Trp-dependent auxin biosynthesis in Arabidopsis: involvement of cytochrome P450s CYP79B2 and CYP79B3. *Genes Dev.* **16,** 3100–12 (2002).

61. Richmond, M. H. THE EFFECT OF AMINO ACID ANALOGUES ON GROWTH AND PROTEIN SYNTHESIS IN MICROORGANISMS. *Bacerial Physiol.* **26,** 398–420

62. Riccardi, G., Sora, S. & Ciferri, O. Production of amino acids by analog-resistant mutants of the cyanobacterium Spirulina platensis. *J. Bacteriol.* **147,** 1002–7 (1981).

63. Kreps, J. A. & Town, C. D. Isolation and Characterization of a Mutant of Arabidopsis thaliana Resistant to α-Methyltryptophan. *Plant Physiol.* **99,** 269–275 (1992).

64. Kreps, J., Ponappa, T., Dong, W. & Town, C. Molecular Basis of a-Methyltryptophan Resistance in amt-1, a Mutant of Arabidopsis thaliana with Altered Try ptophan Metabolism. *Plant Physiol.* **110,** 1159-1165 (1996).

65. Zhao, Y. *et al.* A role for flavin monooxygenase-like enzymes in auxin biosynthesis. *Science* **291,** 306–9 (2001).

66. Barczak, A., Zhao, J., Pruitt, K. & Last, R. 5-Fluoroindole Resistance Identifies Tryptophan Synthase. *Genetics* **140,** 303-313 (1995).

67. Sieburth, L. & Elliot, M. Molecular Dissection of the AGAMOUS Control Region Shows That cis Elements for Spatial Regulation Are Located Intragenically. *The Plant Cell* **9,** 355–365 (1997).

68. Phares, W. & Chapman, L. Anacystis nidulans mutants resistant to aromatic amino Anacystis nidulans Mutants Resistant to Aromatic Amino Acid Analogues. *Journal of Bacteriology* **122,** 943-948 (1975).

69. Sieburth, L. & Meyerowitz, E. Molecular dissection of the AGAMOUS control region shows that cis elements for spatial regulation are located intragenically. *The Plant Cell* **9,** 355–65 (1997).

70. Haughn, G., Davin, L., Giblin, M. & Underhill, E. Biochemical Genetics of Plant Secondary Metabolites in Arabidopsis thaliana. *Plant Physiol.* **97,** 217–226 (1991).

71. Pichersky, E. & Gang, D. Genetics and biochemistry of secondary metabolites in plants: an evolutionary perspective. *Trends Plant Sci.* **5,** 439–445 (2000).

72. Dixon, R. Natural products and plant disease resistance. *Nature* **411,** 843–847 (2001).

73. Dudareva, N. & Pichersky, E. Biochemical and Molecular Genetic Aspects of Floral Scents. *Plant physiol.* **122,** 627–633 (2000).

74. Mol, J., Grotewold, E. & Koes, R. How genes paint flowers and seeds. *Trends Plant Sci.* **3,** 212–217 (1998).

75. Urano, K., Kurihara, Y., Seki, M. & Shinozaki, K. “Omics” analyses of regulatory networks in plant abiotic stress responses. *Curr. Opin. Plant Biol.* **13,** 132–8 (2010).

76. Yamaguchi-Shinozaki, K. & Shinozaki, K. Transcriptional regulatory networks in cellular responses and tolerance to dehydration and cold stresses. *Annu. Rev. Plant Biol.* **57,** 781–803 (2006).

77. Kaplan, F. *et al.* Exploring the Temperature-Stress Metabolome. *Plant Physiol.* **136,** 4159–4168 (2004).

78. Moco, S. *et al.* A Liquid Chromatography-Mass Spectrometry-Based Metabolome Database for Tomato. *Plant Physiol.* **141,** 1205–1218 (2006).

79. Giavalisco, P., Hummel, J., Lisec, J., Inostroza, A. & Catchpole, G. High-Resolution Direct Infusion-Based Mass Spectrometry in Combination with Whole 13 C Metabolome Isotope Labeling Allows Unambiguous Assignment of Chemical Sum Formulas. *Anal. Chem.* **80,** 9417–9425 (2008).

80. Thurman, E.M. & Mills M.S. Solid-phase Extraction: Principles and Practices. John Wiley & Sons, INC. (1998)